A Summary of the Thesis entitled

"Syntheses, Crystal Structures, Magneto-Structural Correlation and Biomimetic Study of Copper(II) Complexes"

To be Submitted

As a partial fulfilment for the award of the degree of

DOCTOR OF PHILOSOPHY

In

Chemistry

By

Mr. Abhay Kumar Patel

Under the supervision of

Dr. R. N. Jadeja

Department of Chemistry

Faculty of Science

Maharaja Sayajirao University of Baroda

Vadodara 390 002

India

April 2021

Summary of the Thesis work

To be submitted to The Maharaja Sayajirao University of Baroda for the award of the degree of DOCTOR OF PHILOSOPHY in Chemistry.

Name of Student: Abhay Kumar Patel

Title of the Thesis: *"Syntheses, Crystal Structures, Magneto-Structural Correlation and Biomimetic Study of Copper(II) Complexes*"

Name of the Supervisor: Dr. R. N. Jadeja
The Maharaja Sayajirao University of Baroda

Faculty: Faculty of Science, The Maharaja Sayajirao University of Baroda.

Department: Department of Chemistry

Registration No.: FOS/2111

Date of Registration: 25th July 2018

Abhay Kumar Patel
Research Student

Dr. R. N. Jadeja
Research Guide

The Thesis work is presented in form of the following chapters:

Chapter 1: Introduction

Chapter 2: Copper(II) complexes with hydrazone blocking ligands

(A) ***Pseudohalidescopper(II) complexes with a hydrazide blocking ligand: Synthesis, spectral characterization and evaluation of antioxidant superoxide dismutase activity***

(B) ***Copper(II) tetrahedral complex derived from N'-[(2E,3Z)-4-hydroxy-4-phenylbut-3-en-2-ylidene]acetohydrazide: Synthesis, molecular structure, quantum chemical investigations, antioxidant and antiproliferative properties***

Chapter 3: Copper(II) complexes incorporating NNN-tridentate hydrazone as proligand

(A) ***Synthesis and structural characterization of Copper(II) complexes with flexible hydrazone: Structural diversity, Hirshfeld analysis, density functional calculations and biological study***

(B) ***Penta-coordinated copper(II) complexes with hydrazide based ligand and imidazole as auxiliary ligand: Synthesis, spectral characterization and SOD mimetic activities***

(C) ***Synthesis, spectral characterization and biomimetic activity of homobinuclearcopper(II) 2-[(E)-phenyl(pyridine-2-yl-hydrazone)methyl]pyridine complexes containing inorganic salts***

Chapter 4: Copper(II) hydrazone complexes with different nuclearties and geometries: Synthesis, structure, spectral properties, electrochemical behaviour, density functional study and *in vitro* catalytic activity

Chapter: 1
Introduction

Copper metal has been known and used tremendously since prehistoric times. The word copper and its symbol Cu is formulated from cuprum. This metal is among the 25 richest elements in the earth's crust. It has performed an important role in industrial, technological and cultural developments in ancient times. Hence, along with iron and gold, copper was one of the first metals used extensively. One of the most extensive and well-established uses of copper is for commercial purposes. The metal and its alloys have been used in a variety of applications because they show several useful qualities including malleability, ductility, strength, corrosion resistance and high thermal and electrical conductivity.

Copper is an essential trace element. It exhibits essential biochemical action either as the nutritional element or a constituent of various exogenously administered compounds in humans. It associates with ceruloplasmin, albumin and other proteins. The participation of copper in human disease has been discussed from a biomedical [1] and a biomedical view [2] concentrating on the molecular physiology of copper transport [3]. Recent interest in copper complexes is developed from their potential application as antimicrobial, antiviral, anti-inflammatory, antitumor agents and enzyme inhibitors.

Copper shows wide coordination chemistry. Its main oxidation state is ranging from 0 to 4 but +1 and +2 oxidation states are most common. Very few copper(III) complexes have been reported. The majority of copper(III) complexes d^8 complexes have square planar geometry and are diamagnetic. Similarly, copper(0) complexes and copper(IV) oxidation states are very rare. The coordination number and geometry around the copper metal center vary with the oxidation state. The common geometries of Cu^1 d^{10} ion are two coordinates linear, three coordinates trigonal planar and four coordinates tetrahedral. The metal Cu(II) d^9 particle is mostly found in an exceedingly tetragonal shape coordination setting [4, 5]. Although, four-coordinate tetrahedral and square planar complexes are according [6].

Copper is a crucial trace element, but excessive quantities are toxic to humans [7]. About 2-5 mg of copper is absorbed per day from the diet. Copper deficiency can develop if there is insufficient nutritional copper and show low blood cell counts and osteopenia (low bone density). Though, copper deficiency is rarely seen in developed countries. Sometimes severe copper deficiency noticed like those examined in genetic disorder, Menkes disease [8]. This disease mainly happens in boys since it is X-linked and generally apparent at birth. Such babies are born premature and have unusual appearances and have brain damage that causes mental retardation. For the treatment of such disease metal-based drugs are useful. One of such useful drugs is copper-histidine complexes which may be prescribed. For this drug, clinical trials are underway. Also, chronic toxicity is seen in some individuals. The excessive accumulation of copper damages the liver and then the nervous system and other organs. The dominant, relatively rare disorder is called Wilson's disease [8]. This disease is generally identified in infants too young adults with liver and neurological problems. Wilson's disease is curable with anti-copper agents including zinc acetate (Galzin^{Tm}) which blocks copper absorption and has the lowest rate of side effects or D-penicillamine (Cuprimine, depen) or trientine (suprine) to chelate and remove the excess copper. Tetra thiomolybdate is also being considered to cure this disease and at present is in the phase of the final clinical trial. The roles of copper in other diseases have also been investigated. For Alzheimer's disease cases, it is

observed that amylase protein interacts with copper to produce increased oxidant damage and little amount of copper causes the precipitation of the amyloid β-protein on copper and its complexes.

Alzheimer's [8] disease is a neurological condition in which the death of brain cells causes memory loss and a person may experience difficulty with reasoning, complex tasks and judgment. The drug Nomenda (Memantine) and N-methyl D-aspartate antagonist is prescribed to Alzheimer patients. It is believed to work by regulating glutamate which is an important brain chemical. When produced in excess amount, glutamate may lead to brain cell death. The lowering of copper levels causes to produce antiangiogenesis (retardation of blood vessel growth) and proliferation and hence, is being probed for its potential anticancer effect. Thus, copper lowering agent tetrathiomolybdate is recently involved in several clinical trials for a variety of cancers.

The evolution in the field of bio-inorganic chemistry has aroused interest in Schiff base copper complexes, as long as it has been admitted that many copper(II) Schiff base complexes may serve as models for biologically important species. Schiff bases are formed when primary amine reacts with aldehydes or ketone under specific conditions. Therefore, Schiff base is an analog of aldehydes or ketone in which the carbonyl group has been replaced by an imine or azomethine group (Fig. 1). These Schiff base compounds are easily synthesized and form complexes with almost all metal ions. There are several reports on their applications in biology together with medicine, antifungal, anticancer, inhibitor, an anti-inflammatory drug, an antimalarial drug, antiviral activity and conjointly as catalysts in many reactions. Some major importance of Schiff base copper(II) complexes are given as:

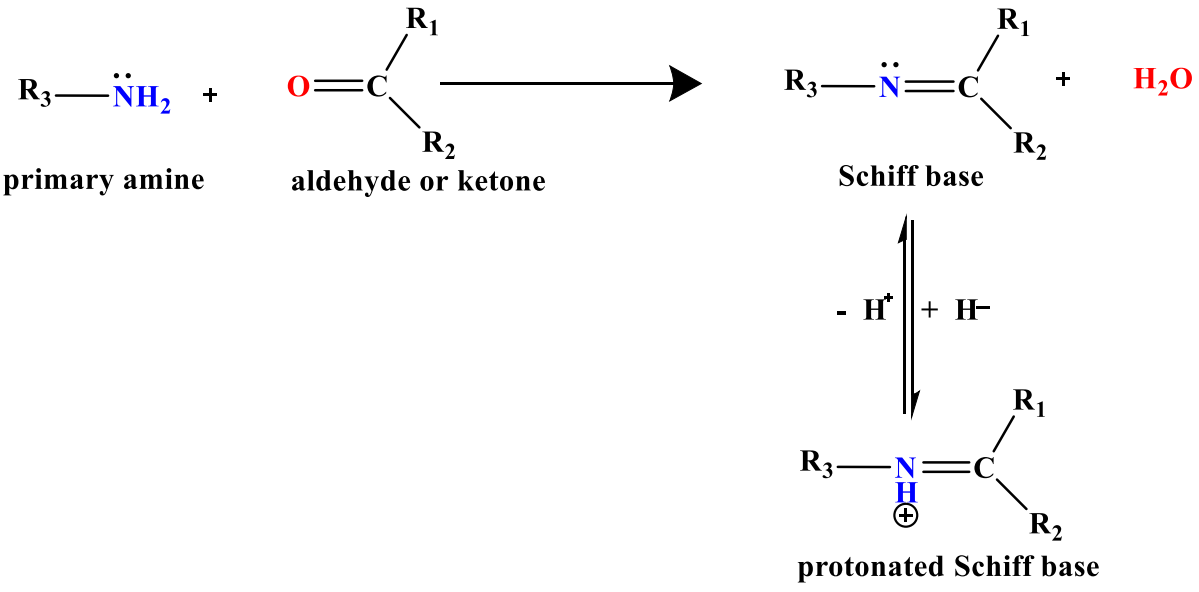

Fig. 1. The general strategy for the synthesis of Schiff base.

Aims and objective of work

The aim of this thesis work has been the synthesis and characterization of new Schiff base ligand and copper(II) complexes. It is immense to synthesize and characterize new small molecular weight copper(II) complexes that mimic the enzyme activity and that assist to explain the structural and electronic features. These features can be varied by changing the ligand and the presence of substituents. The above objective has been obtained with the

synthesis, characterization and use of new mono and bi-nuclear copper(II) complexes with active redox centers. The modulation of ligand structure has a great influence on the physicochemical properties of the complexes. Emphasis is given by collecting quantum chemical parameters and SOD activity data of all synthesized complexes. Nowadays quantum chemical method has become a common and useful tool for the prediction of the structure and properties of complexes. During the tenure of this work, various copper(II) complexes have been synthesized. These complexes were characterized using micro-analysis, molecular mass analysis, spectral (UV-Vis, IR and epr) and electrochemical techniques. Finally, molecular structures of these complexes were obtained from single-crystal X-ray analysis. Quantum chemical calculations (DFT) were also performed to verify the experimental bond parameters. Biological activity (SOD) and anticancer of these complexes have also been explored.

Chapter: 2

Copper(II) complexes with hydrazone blocking ligands

(A) Pseudohalides copper(II) complexes with a hydrazide blocking ligand: Synthesis, spectral characterization and evaluation of antioxidant superoxide dismutase activity

In this chapter, our aim is the synthesis and spectral characterization of copper(II) complexes with hydrazone and pseudo halides as co-ligands. The coordination sites of copper(II) ion prefer square pyramidal geometry, which is generally blocked by tridentate Schiff bases. To saturate the coordination number of the copper(II) ion a bridging ligand *viz* (N3, NCS, NCO) is used. Several transition metal complexes with tridentate and bridging ligands (pseudo halides) have already been reported. These pseudohalides bridged complexes have got diverse structures and potential applications in magnetic materials. Pseudo halide ligands can coordinate to transition metal ions in different ways. In this chapter using (E)-N'-(phenyl(pyridin-2-yl)methylene)thiophene-2-carbohydrazide (HL) ligand, four copper(II) mono and binuclear complexes like $[Cu(L)(ClO_4)(H_2O)]$ (**1**), $[(Cu)(L)(N_3)]_2$ (**2**), $[(Cu)(L)(OCN)]_2$ (**3**), and $[(Cu)(L)(CNS)]_2$ (**4**) have been synthesized and characterized using UV-vis, infrared and Epr spectroscopic techniques. The electrochemical behaviour of these complexes was also studied using cyclic and differentials pulse voltammetry (CV and DPV). Additionally, the antioxidant superoxide dismutase (SOD) activity of these complexes has been also evaluated.

Experimental

Synthesis of ligand (HL)

The pro-ligand was synthesized by condensing thiophene-2-carboxylic acid hydrazide (0.71 g, 10 mmol) with 2-benzoyl pyridine (0.96 g, 10 mmol) in ethanol 40 mL according to the procedure as reported previously (Scheme 1). The reaction mixture was refluxed for 3 hrs. The resulting solution was filtered and filtrate left for evaporation at RT, whereas solid mass was obtained. M.P.: 125 °C. Yield ~ 80 %. Molecular Weight: 307.37. Anal. Calc. for $C_{17}H_{13}N_3OS$: C, 66.43; H, 4.26; N, 13.67 %. Found: C, 66.49; H, 4.24; N, 13.69 %. FTIR (KBr, cm^{-1}): ν(NH) 3174, ν(OH) 3306, ν(C=O) 1645, ν(C=N) 1604. ^{1}H NMR (DMSO-d_6, 400MHz) δ: 11.3 (s, 1H, -NH-), 9.1 (s, 1H, -CH=N-), 8.9 (s, 1H, -CH-S-), 8.5-7.1 (m, 10H, Ar-H) ppm. ^{13}C NMR (DMSO-d_6, 400MHz) δ: 185.9 (C=O), 156.8 (Ar-C, -C=C), 149 (-CH=N), 138.1 (-CH-S), 148-116 (Ar-C) ppm.

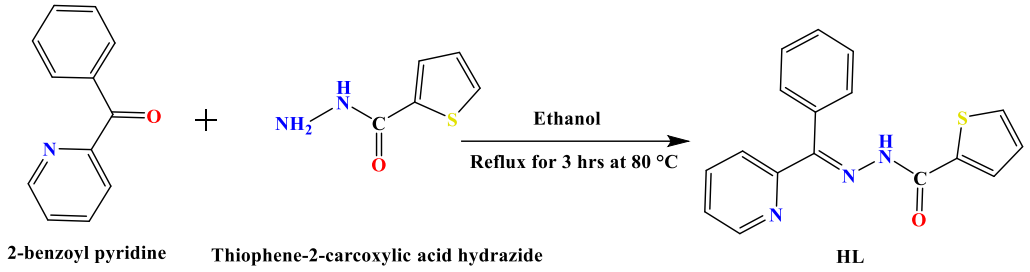

Scheme 1 Synthesis of hydrazone ligand **HL**.

Synthesis of complex [Cu(L)(ClO$_4$)(H$_2$O)] 1

To a 10 mL methanolic solution of Cu(ClO$_4$).6H$_2$O (0.370g, 1 mmol) was added 10 mL methanol solution of HL (0.307g, 1 mmol) and stirred for 1 hrs. The mixture was filtered and the filtrate was left for evaporation at room temperature. After one-week blue coloured complex separated. The product was collected by filtration, washed with cold methanol and stored in calcium chloride desiccators. Yield ~ 74 %. Molecular Weight: 487.37. Anal. Calc. for $C_{17}H_{14}ClCuN_3O_6S$: C, 41.88; H, 2.89; N, 8.61 %. Found: C, 41.90; H, 2.90; N, 8.62 %. FTIR bands (KBr, cm^{-1}): ν(C=N) 1575, ν(C−O^{-}) 1292**,** ν(ClO$_4^-$) 1073. ESI-Mass (m/z): 487.12.

Similarly, all other complexes **2-4** were synthesised using same procedure as complex **1**. The synthetic route of complexes is given in scheme 2.

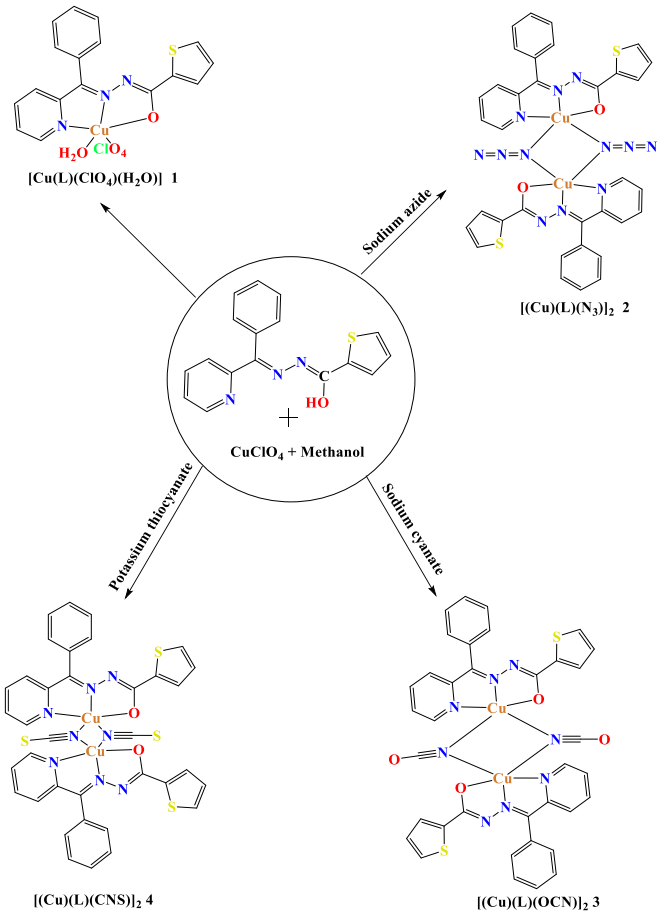

Scheme 4 Synthetic route of complexes **1-4**.

Results and Discussion

NMR spectra of ligand

The ^{1}H NMR and ^{13}C NMR of ligand were recorded in DMSO-d_6 solvent. The NMR spectra of the ligand give the right information of the ligand structure. In ^{1}H NMR of ligand we find a singlet peak at 11.3 ppm is due to hydrazide (-NH-) proton. Similarly, azomethine (-CH=N-) proton peak is observed at 9.1 ppm and (-CH-S) peak is obtained at 8.9 ppm. All other aromatic protons peaks are observed in the range of 8.5-7.1 ppm. ^{1}H NMR spectrum is shown in (Fig. 1). In ^{13}C NMR spectra, we find that carbonyl carbon peak at 185.9 ppm, (C=C) peak is obtained at 156 ppm, Similarly, azomethine carbon peak at 149 ppm and (CH-S) carbon peak is obtained at 138.1 ppm. All other aromatic carbon peaks are observed in the range of 156-116 ppm. ^{13}C NMR spectrum is shown in (Fig. 2).

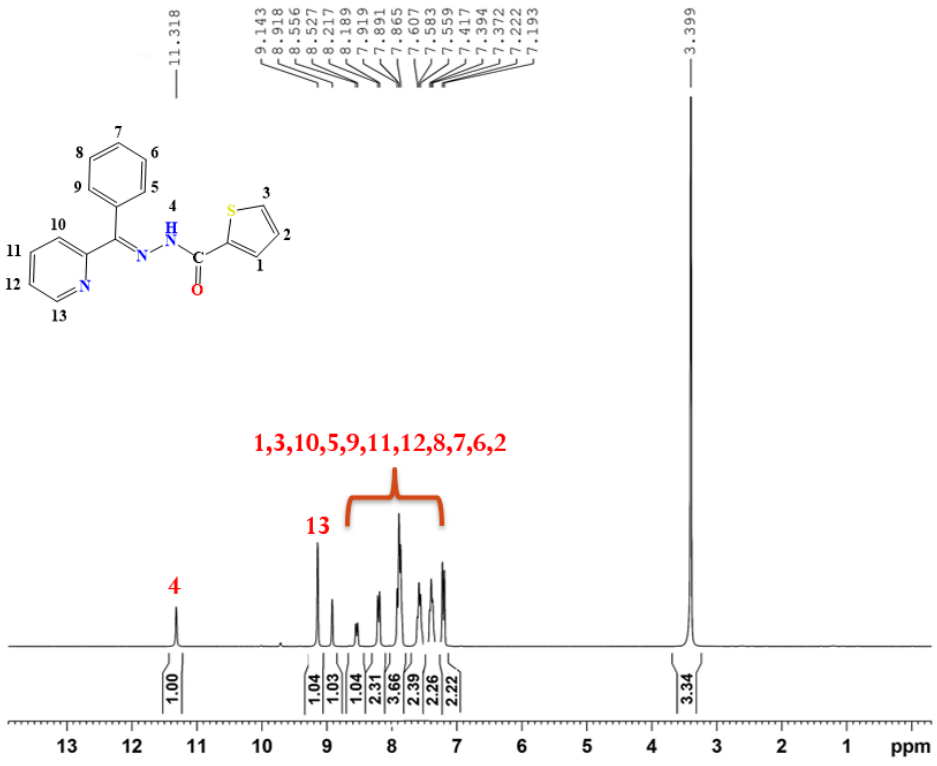

Fig. 1. ^{1}H NMR of ligand **HL**.

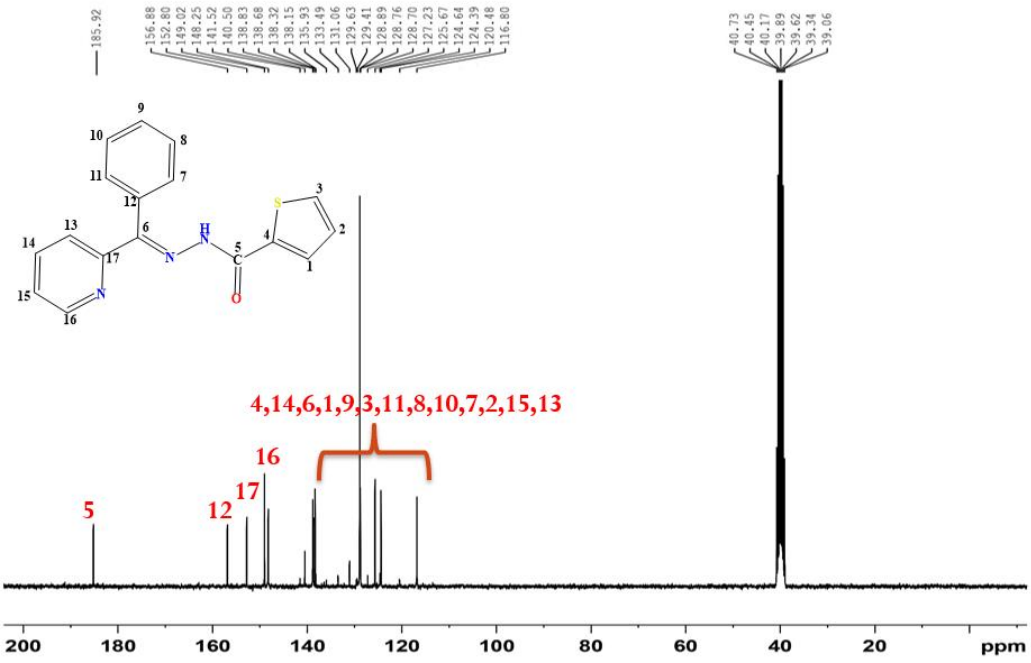

Fig. 2. ^{13}C NMR of ligand **HL**.

FTIR Spectra

FTIR spectra of complexes (**1-4**) were analysed in comparison to free unbound ligand (HL). The FTIR spectrum of the HL shows a band ~ 3174 cm^{-1} due to ν(N-H) and ν(OH) at 3306 cm^{-1}. The FTIR band at ~1604 cm^{-1} indicates the presence of the ν(>C=N) group. The FTIR spectra of complexes (**1-4**) show absorption bands in the 1572-1599 cm^{-1} region, which can be assigned to the >C=N stretching frequency of the coordinated L. The shift of this absorption band on complexation towards lower wave number reveals the coordination of the azomethine nitrogen to the copper centre. The absence of 3174 ν(N−H) and ν(C=O) bands and appearance of a new ν(C−O^{-}) band in the range 1292-1285 cm^{-1} in all the metal complexes indicate that the ligand enolizes during complexation and bonding occurs through a deprotonated enolate-O with metal. Complex **1** shows a band at 620 and 1100 cm^{-1} due to coordinated perchlorate anion to copper centre. The band observed at 3418 cm^{-1} in **1** is due to coordinated water. FTIR spectrum of the complexes showed a strong absorption band at 2018 cm^{-1}indicating azido ligand, sodium cyanate at 2016 cm^{-1} and a band at 1959 cm^{-1} indicating thiocyanate ligands [51]. The FTIR spectrum of complexes shows two bands at 2110 and 2138 cm^{-1} indicating the presence of bridging thiocyanate. The ligand coordination to the copper centre is confirmed by two peaks are seen in IR spectrum of each complex, at 406-491 cm^{-1} and 423-467 cm^{-1} due to ν(Cu-N) and ν(Cu-O) respectively.

Electronic spectra

The electronic spectra of complexes recorded in DMSO solutions (3.0×10^{-3}M) of all complexes. The absorption band observed in the range 402-405 nm may be attributed to the ligand-to-metal charge transfer (LMCT) transition for each complex (Fig. 8). In the visible region, all complexes display a single absorption band in the range 680-705 nm, agreeing with the expected five-coordinate geometry around copper center. Complex **1** shows the band at 660 and the other shows at 725 nm this difference in band position is due to the mono and binuclear

nature of complexes. One more absorption band found at ~300 nm in all complexes is consistent with the π-π*/n- π* transition. This highest energy transition is ligand based. In general five coordinate copper(II) complexes possess square pyramidal or distorted square pyramidal geometry, whereas the corresponding trigonal bipyramidal complexes generally show a maximum at >>800 nm with a higher energy shoulder. In present complexes observed d-d bands remain the range 680-725 nm indicating the distortion in square pyramidal geometry. This absorption maxima present in the visible region arises from a $^2E \rightarrow {}^2T_1$ transition.

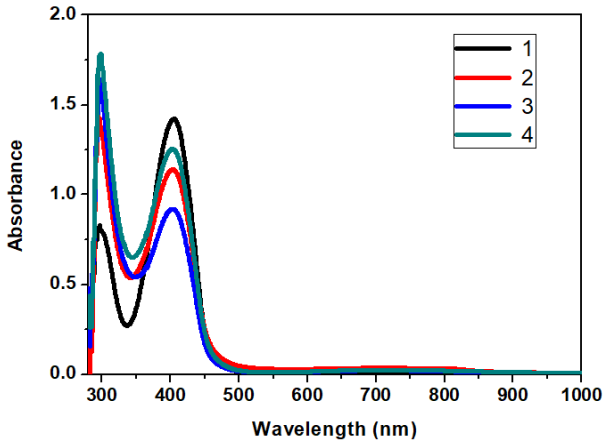

UV-visible spectra of copper(II) complexes **1-4** in 3.0 × 10^{-3} M DMSO solution.

Epr studies

X-band epr spectra of four new copper(II) complexes were recorded of polycrystalline samples at room temperature (RT) and liquid samples in DMSO (3.0 × 10^{-3} M) at liquid nitrogen temperature(LNT). Epr spectra are shown in and epr spectral parameters are collected in Table 2. For complex **1**, the spectrum of the polycrystalline sample at RT is broad and almost isotropic. This yields two signals $g_{\|}$ = 2.224 and$g_{\perp}$= 2.205. The exchange interaction parameter (G) for this complex is 4.21 indicating no interaction between two dipolar units. Polycrystalline spectra of remaining complexes **2-4** show the polycrystalline spectra with the well-defined half-field signal in the range 1560-1535 G. The presence of such a half-field signal resembling the characteristic signals of exchange-coupled complexes. The G value of these complexes is also less than 4, revealing the interaction in between two dipole units. As these complexes are binuclear, therefore the nature of the interaction is dipole-dipole intramolecular interaction. The bandwidth (ΔB_{pp}) of the perpendicular component is also estimated and given in Table 2. The ΔB_{pp} allows a better evaluation of exchange interaction. The value of ΔB_{pp} for **1** is 140 G and for remaining complexes ~105 G. The reduced ΔB_{pp} of complexes **2-4** also reveals exchange interaction. Low temperature solution spectra of all complexes were also measured in frozen DMSO solution. Complex **1** shows well-resolved esr spectrum with $g_{\|}$ = 2.210 and $g_{\perp}$= 2.068 corresponding to mononuclear complexes with $g_{\|} > g_{\perp} > 2.0023$. The overall epr spectral features are almost similar for the remaining three complexes (**2-4**). In epr spectra, all three complexes $g_{\|}$ region show six $g_{\|}$ signals. The presence of six $g_{\|}$ signals indicates that the binuclear complex dissociates in solution. Therefore, each spectrum results from the overlap of two species, as is evident in $g_{\|}$ region and parameters are collected in Table 2.

Spin Hamiltonian parameters for complexes **1-4**.

Complex	RT (Polycrystalline)				LNT (Solution)				
	$g_{\parallel}$	$g_{\perp}$	G	ΔB_{pp}(G)	$g_{\parallel}^{1}$	$g_{\parallel}^{2}$	$A_{\parallel}^{1}$(G)	$A_{\parallel}^{2}$(G)	$g_{\perp}$
1	2.224	2.055	4.21	140	2.210	-	160	-	2.068
2	2.210	2.055	3.89	103	2.241	2.203	157	159	2.067
3	2.218	2.068	3.281	105	2.233	2.203	170	170	2.058
4	2.218	2.061	3.61	107	2.207	2.213	160	160	2.065

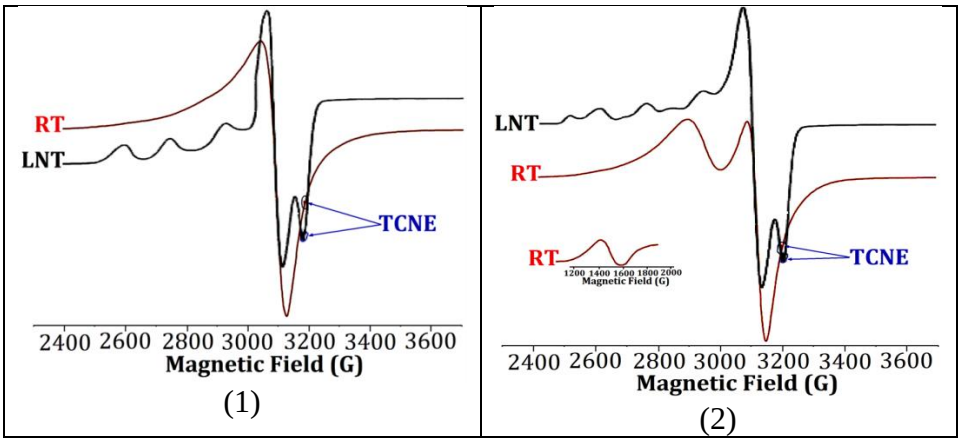

Epr spectra of complexes in RT and LNT **1** and **2.**

Electrochemical Activity

Electrochemical properties of complexes **1-4** were studied using cyclic voltammetry (CV) and differential pulse voltammetry (DPV) in DMSO solution containing 0.1M tetra butyl ammonium perchlorate (TBAP). All complexes show two reduction potentials corresponding to two separate couples (1) and (2) in:

$$Cu^{II}\,Cu^{II} \rightleftharpoons Cu^{II}\,Cu^{I} \qquad (1)$$

$$Cu^{II}\,Cu^{I} \rightleftharpoons Cu^{I}\,Cu^{I} \qquad (2)$$

The anodic counterparts of these redox waves are not well defined. The peak potentials beyond these equations (1) and (2) are due to the reduction of ligand moiety of complexes.

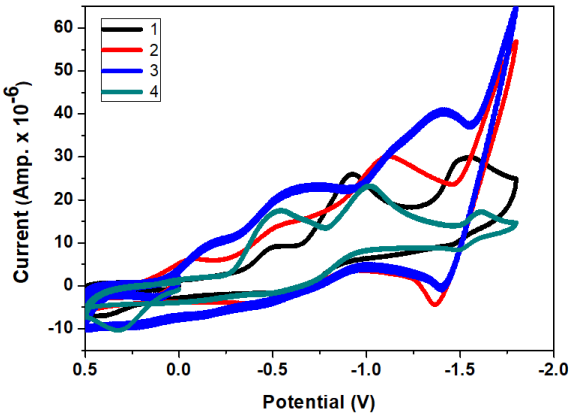

Cyclic voltammograms for complexes **1-4** in DMSO at an Ag/AgCl electrode with scan rate 100 mVs^{-1} and temperature of 25˚C.

DFT Calculations

B3LYP estimated interatomic distances and bond angles of **1-4** are given in Table. All calculations were performed with the GAUSSIAN09 program, with the aid of the Gauss View visualization program. The coordination polyhedron of Cu atom is a distorted square pyramid in **1** with 3N 1O in the equatorial plane and 1O 1N in axial position. whereas in binuclear complexes **2-4** each Cu atom is surrounded to 2N2O in equatorial and 1 O in axial position. The distorted square pyramidal geometry (τ_5 = β-α / 60° =0.288) of copper(II) ion in **1** is recognized by four bond lengths Cu(23)-O(21) = 1.839, Cu(23)-O(24) = 1.829, Cu(23)-N(2) = 1.877 and Cu(23)-N(14) = 1.864 Å at equatorial plane and Cu(23)-O(41) = 1.828 Å at axial position. Likewise, the coordination geometry of each copper centres in **2-4** may be described as a distorted square pyramid, as evidenced by the low value of the geometrical structural index (τ_5). The geometrical structural index (τ_5) falls in the range 0.01-0.117. The distortion in polyhedron results from the Jahn-Teller Cu^{2+} ions with d^9 configuration which is typical of a square-based pyramidal geometry. The slightly distorted square geometry of each copper(II) centers in these complexes (**2-4**) is in good agreement with the structural data (bond lengths and bond angles). The Cu-N equatorial distances remain in a range of 1.784-1.899 Å whereas Cu-O equatorial distances fall in a range of 1.862-1.877 Å in complexes (**1-4**). The Cu-Cu distances found to be 2.047, 2.192 and 1.187 Å for **2**, **3** and **4** respectively.

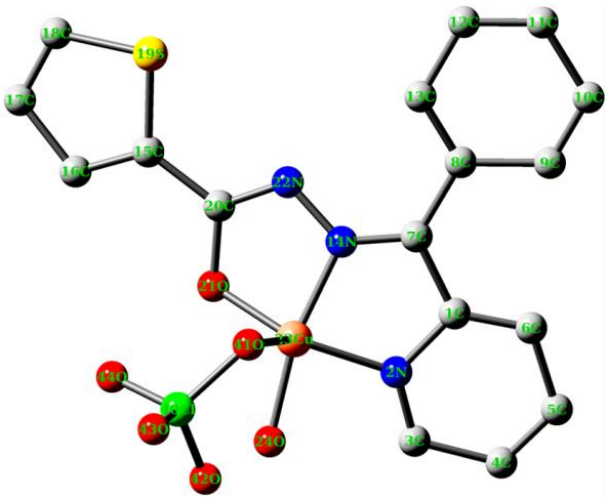

Optimized structure of complex **1**.

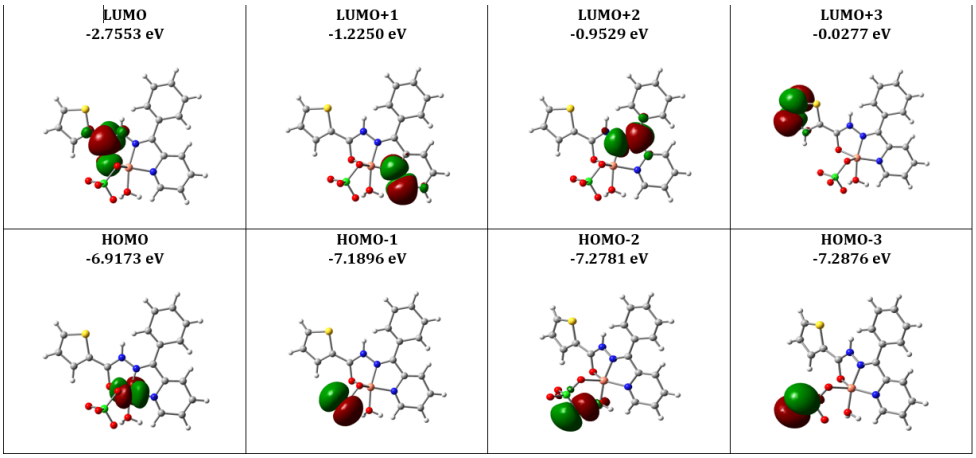

HOMO-LUMO analysis of complex **1**.

Catalytic activity

All the synthesized mono and binuclear complexes exhibit catalytic activity towards the dismutation of superoxide anions at physiological pH. The superoxide dismutase (SOD) catalytic activities were carried out in a phosphate buffer of pH 7.8 by the NBT assay method. The concentrations of catalysts required to yield 50% inhibition of the reduction nitro blue tetrazolium chloride (NBT) defined as IC_{50} were calculated. The catalytic parameters compared to the similar systems of biologically important ligands as well as values of best SOD mimics reported in the literature are also given for comparison point of view. The relative high SOD activity of complexes **1-4** show good SOD activity may be attributed to the flexible nature of hydrazone ligand, which can facilitate the reduction of copper(II) to copper(I) associated with variation of coordination geometry and the accommodation of copper(I).

The SOD activity, IC_{50} values and k_{McCF} values for complexes **1-4**.

Complex	IC_{50}(µmol)	SOD activity (µmol^{-1})	k_{McCF} (mol L^{-1}) S^{-1}	Ref.
1	20	50.00	16.63	This work
2	24	41.666	13.86	This work
3	34	29.411	9.78	This work
4	30	33.333	11.09	This work
$[Cu_2(\mu\text{-}SCN)_2(L)_2]$	24	41.66	13.86	78
$[(L^1)Cu(\mu\text{-}CH_3COO)_2Cu(L^1)]$	35	28.57	9.50	70
$[(L^1)Cu(\mu\text{-}NO_3)2Cu(L^1)]$	26	38.46	12.79	91
Vc	852	1.17	0.39	92

Where L = N'-[(Z)-phenyl(pyridin-2-l)methylidene]acetohydrazide, L^1 = N'-[(E)-phenyl(pyridin-2-yl)methylidene]benzohydrazide.

4 Conclusions

In this chapter, we have reported the synthesis of a new Schiff base ligand, N'-(phenyl-pyridine-2-yl-methylene)-thiophene-2-carboxylic acid hydrazide (HL) and its metal complexes. The ligand and its complexes are well characterized by analytical and spectral method. The molar conductance values of the complexes 1-4 in DMSO at room temperature are observed in the range 8.34–18.24 (Ω^{-1} cm^2 mol^{-1}) indicating that they are non-electrolytes nature. The distorted square pyramidal geometry ($\tau_5 = \beta\text{-}\alpha/60° = 0.288$) of copper(II) ion in complex **1** the

coordination geometry of each copper centres in **2-4** may be described as a distorted square pyramid, as evidenced by the low value of the geometrical structural index (τ_5). The geometrical structural index (τ_5) falls in the range 0.01-0.117 in complexes **2-4**. The distortion in polyhedron results from the Jahn-Teller Cu^{2+} ions with d^9 configuration which is typical of a square-based pyramidal geometry. The G value of these complexes is also of less than 4, revealing the interaction in between two dipole units. As these complexes are binuclear in nature, therefore the nature of interaction is dipole-dipole intramolecular interaction. The catalytic rate constant (k_{McCF}) was also calculated for all complexes. The k_{McCF} value of **1-4** are 16.63, 13.86, 9.78 and 11.09 respectively. On perusal of k_{McCF} values, it is clearly indicated that **1-4** can be used as an antioxidant superoxide scavenger.

Chapter: 2

(B) Copper(II) tetrahedral complex derived from N'-[(2E,3Z)-4-hydroxy-4-phenylbut-3-en-2-ylidene]acetohydrazide: Synthesis, molecular structure, quantum chemical investigations, antioxidant and antiproliferative properties

In this part of thesis one copper(II) complex using HL = N'-[(2E, 3Z)-4-hydroxy-4-phenylbut-3-en-2-ylidene]acetohydrazide was synthesized. This complex was synthesized and characterized by various physicochemical techniques. The solid-state structure has been determined using single-crystal X-ray analysis. The geometry for this complex has been pseudo tetrahedral τ_4 = 0.81. The density functional theory was used to compute the molecular structure, HOMO-LUMO and natural bond order (NBO) analysis. The binding of the Schiff base to the copper(II) has been explored using X-band epr spectral measurements. Similarly, electrochemical behavior has been studied using cyclic voltammetry and differential pulse voltammetry. The antioxidant SOD activity has been collected. Antiproliferative and cancer properties in vitro of the complex have also been collected using human cancer cell lines including human cell lines, IMR 32 (Neuroblastoma), MCF 7 (Breast cancer), HepG2 (Hepatocellular carcinoma) and L132 (lung cells).

Experimental

Synthesis of ligand HL

To a solution of 1-benzoyl acetone (1.62 g, 10 mmol) in absolute ethanol (50 ml), acetyl hydrazide (0.7 8g, 10 mmol) was added. The resulting solution was refluxed at 75 °C for 3 hrs. The yellowish solution was filtered and the filtrate was kept for slow evaporation at room temperature to yield a light-yellow polycrystalline sample. The Schiff base was washed with ethanol and dried over fused $CaCl_2$.

M.P.: 125 °C. Yield: ~ 78 %. Anal. Calc. for $C_{12}H_{14}N_2O_2$ (218.26 g mol^{-1}): Elemental Analysis: C, 66.07; H, 6.47; N, 12.86 %; Found: C, 66.06; H, 6.48; N, 12.84 %. FTIR bands (KBr, cm^{-1}): ν(C=O) 1601, ν(C=N) 1571. ^{1}H NMR (DMSO-d_6) δ: 12.1 (s, 1H, OH), 10.3 (s, 1H, -NH-), 7.8-7.3 (m, 6H, Ar-H), 2.2 (s, 2H, C-CH_3), 1.99 (s, 3H, CH_3) ppm. ^{13}C NMR (DMSO-d_6) δ: 169 (C-OH), 154 (C=O), 144 (CH=N-), 131-91 (Ar-C), 23.3 (-CO-CH_3), 16.1 (CH-CH_3) ppm.

Synthesis of Complex [Cu(HL)(NO_3)]

The Schiff base ligand (0.281g, 1.0 mmol) was dissolved in methanol (20 mL). A solution of $Cu(NO_3)_2.3H_2O$ (0.241 g, 1.0 mmol) in methanol (20 mL) was added dropwise to the above solution with stirring for 5 hrs to give a green clear solution. The resulting solution was filtered. The filtrate was left for slow evaporation at room temperature. Plate-like crystals were formed from the solution two weeks later. These crystals were washed with hot distilled water and then ethanol to remove impurities. The crystals were dried under a vacuum.

Yield: ~ 73 %. Anal. Calc. for $C_{12}H_{13}CuN_3O_5$ (342.79 g mol^{-1}): Elemental Analysis: C, 43.62; H, 4.51; N, 11.51; Found: C, 43.65; H, 4.52; N, 11.78. FTIR bands (KBr, cm^{-1}): ν(C=O) 1593, ν(C=N) 1563. ESI-Mass (m/z): 344.18.

Results and discussion

The copper(II) complex was synthesized using 1-benzoyl acetone and acetyl hydrazide as a ligand (Scheme 1). The complex [Cu(HL)(NO_3)] has been synthesized by a general procedure based on mixing a methanolic solution of copper nitrate with a methanolic solution of the ligand in a 1:1 molar ratio Scheme 2. The complex has been characterized by FT-IR, UV-Vis, CV, ESI-Mass, Hirshfeld analysis and X-ray analysis. The SOD and anti-cancer activity of complex have been also evaluated.

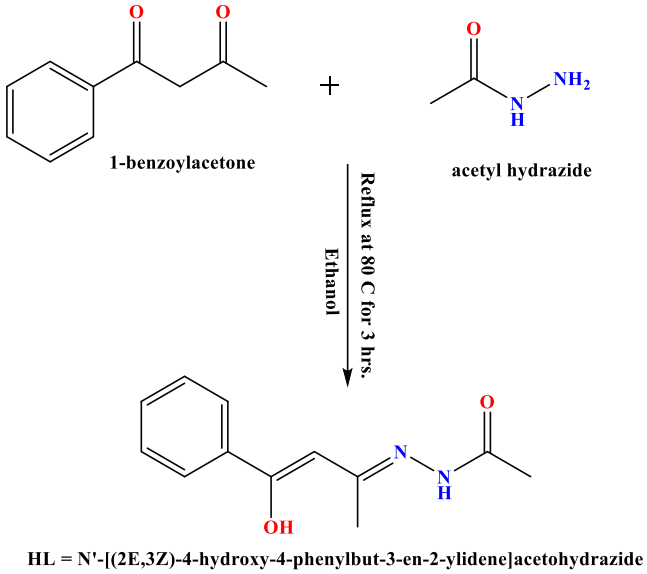

Scheme 1 Synthetic route for the preparation of the ligand (**HL**).

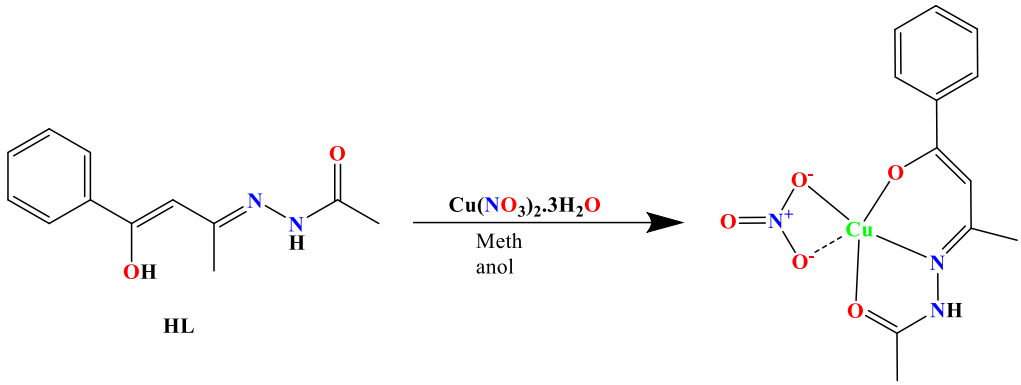

Scheme 2 Synthetic route of the complex **[Cu(HL)(NO_3)]**.

NMR spectra of Ligand

The ^{1}H and ^{13}C NMR spectra of ligand (HL) were recorded in DMSO-d_6 solvent. In ^{1}H NMR of spectra of ligand hydroxy (-OH) peak is obtained at 12.1 ppm. The NH peak is obtained at 10.3 ppm. All aromatic peaks along with aliphatic are obtained at the range of 7.8-7. ppm. Two methyl peaks are obtained at 1. and 2.2 ppm. In ^{13}C NMR (C-OH) peak and carbonyl (C=O), carbon peaks are obtained at 169 and 154 ppm. Similarly, azomethine carbon (CH=N) peak is obtained at 144 ppm. All other carbon peaks are obtained at 131-92 ppm. Two methyl carbon peaks are obtained at 16 and 23 ppm.

Crystal structure of complex

An ORTEP view of the complex with its atom numbering scheme is shown in Fig. This complex crystallizes in the triclinic space group (*P*-1). The copper(II) centre in this complex is four coordinated by two oxygen atoms (O1 and O2) and one nitrogen atom (N1) of the Schiff base and one oxygen atom (O3) of the nitrate ligand, forming a pseudo tetrahedral geometry. The oxygen atom of nitrate is weakly coordinated with copper(II) centre. In this complex, the Cu(II) centre in an approximate pseudo-tetrahedral geometry is ascertained by the value of τ-index ($\tau_4 = 360^0 - (\alpha + \beta) / 141^0$), where α and β are the two largest angles in four coordinate complexes. The value of τ_4 would range from 1.00 for a perfect tetrahedral geometry to zero for a perfect square planar geometry. For this complex τ_4 is 0.81. Therefore, the geometry of copper ions is approximately tetrahedral.

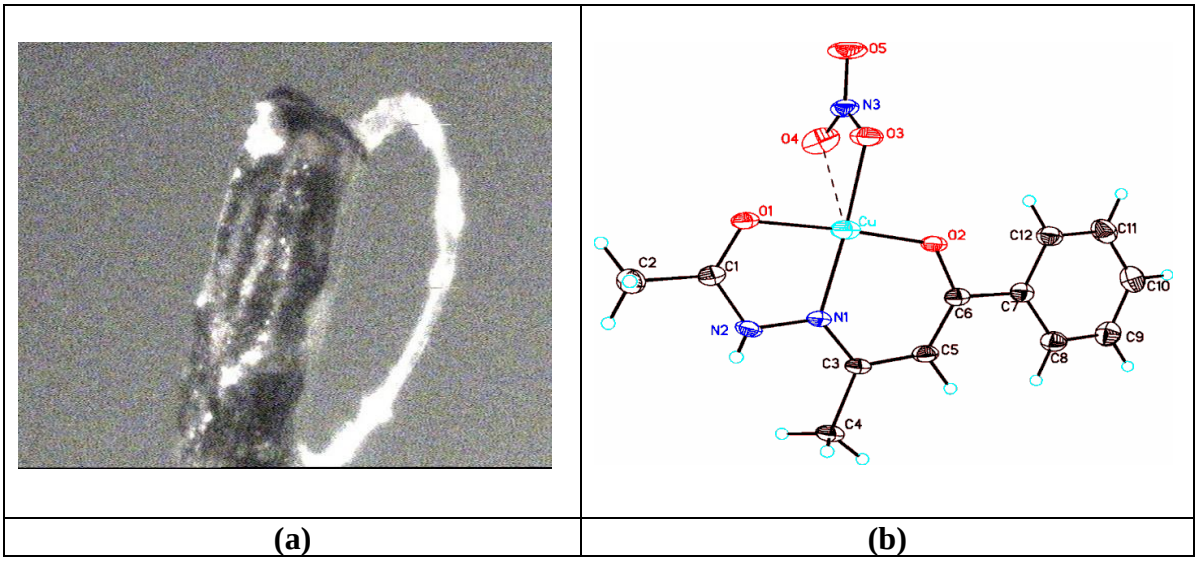

(a) **(b)**

Crystal image and **(b)** ORTEP view of the complex [Cu(L)(NO_3)].

DFT based frontier orbital analysis

The six important α and β molecular orbitals (MOs), viz., HOMO-2, HOMO-1, HOMO, LUMO, LUMO+1 and LUMO+2 were analysed for the present complex. HOMO (highest occupied molecular orbital) and LUMO (lowest occupied molecular orbital) are collectively referred to as frontier orbitals and are important parameters for describing chemical behaviours. The HOMO orbitals are primarily electron donors whereas LUMO is electron acceptors. Similarly, the gap between HOMO and LUMO describes the chemical stability of molecules. The computed energies of six α-spin state molecular orbitals (HOMO-2 to LUMO+2) for the complex are -5.440 eV, -5.368 eV, -4.730 eV, -5.795 eV, -4.051 eV and -0.996 eV respectively and energy gap (ΔE) between (HOMO – LUMO), (HOMO-1 – LUMO+1), (HOMO-2 – LUMO+2) for the complex are 1.065 eV, 1.317 eV and 4.444 eV respectively. Similarly, six MOs energies of β-spin states (HOMO-2 to LUMO+2) are also estimated for the complex viz., -5.437 eV, -9.307 eV, -4.765 eV, -5.790 eV, -5.088 eV and 1.086 eV while the energy gap between (HOMO – LUMO), (HOMO-1 – LUMO+1), (HOMO-2 – LUMO+2) are 1.025 eV, 0.219 eV and 4.351 eV respectively.

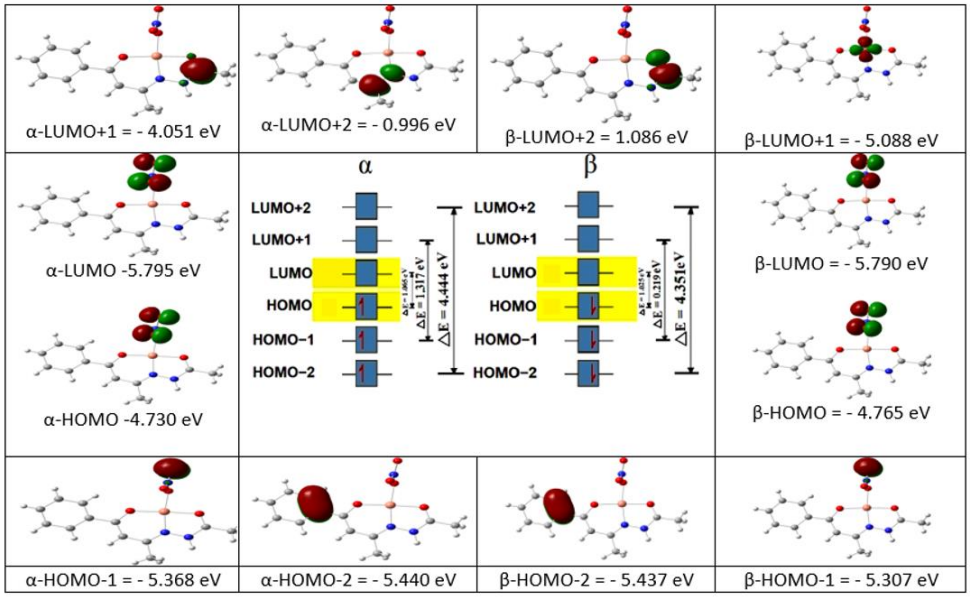

HOMO-LUMO structure with energy level diagram of complex [Cu(L)(NO_3)].

Natural bond orbital (NBO) analysis

The NBO analysis of complex was done by B3LYP/LANL2DZ level basis set. The observed bond lengths and angles exactly tally with the experimentally observed values. The NBO analysis is used to predict the delocalization of electron density between occupied Lewis-type orbitals and unoccupied non-Lewis NBOs (Rydberg), which correlate to a stabilizing donor-acceptor interaction. As per NBO analysis, all of the interactions between the copper(II) ions and all of the nitrogen and oxygen donor atoms were regarded as coordination bonds (N→Cu or O→Cu). Such type of interactions attribute to a donation of the electron density from the lone pair orbital on the nitrogen or oxygen atoms, LP(N) or LP(O) to the antibonding orbital on the copper ion $LP^*(Cu)$. The selected orbitals involved in the strongest LP(N) → $LP^*(Cu)$ and LP(O) → $LP^*(Cu)$ interactions are depicted. The natural atomic configuration for Cu^{2+} = +0.641, O_1 = -0.431, O_2 = -0.324, O_3 = -0.294 and for N_1 = -0.323. Similarly, natural electronic configuration of Cu is: [Core] 4s (0.31) 3d (9.35) 4p (0.34) and natural population analysis of Cu is: core electrons (17.9954), valence electrons on 4s, 4p and 3d orbital (9.9979) and Rydberg electrons on 4p, 4d and 5p orbitals (0.01047) give 27.99338 electrons. Before complexation, the charge on copper is +2, while the charge of the copper(II) ion in complex is +0.641. These shows that ligand transfer own negative charge to copper(II) ion during complex formation.

Donor	Acceptor	Interaction
LP(N)	$LP^*(Cu)$	LP(N)→ $LP^*(Cu)$
LP(O)	$LP^*(Cu)$	LP(O)→ $LP^*(Cu)$

The donor and acceptor orbitals involved in the LP(N) → $LP^*(Cu)$ and LP(O) → $LP^*(Cu)$ interactions [Cu(L)(NO_3)].

Hirshfeld Surface Analysis

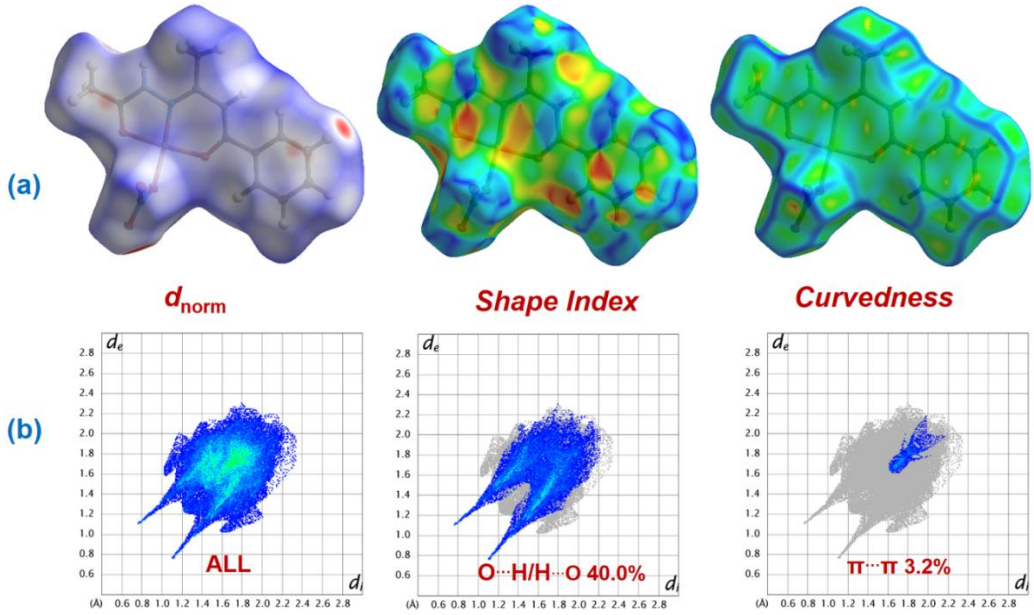

(a) Hirshfeld surfaces mapped with d_{norm}, shape index and curvedness for the complex; **(b)** Fingerprint plots for the complex showing percentages of contact contributed to the total Hirshfeld surface area in the complex.

FTIR spectroscopy

The FTIR spectrum of the complex was analyzed in comparison with that of free ligand (HL) in the region 4000-400 cm^{-1}. The IR data gave the evidence for the coordination of ligand (HL) to the copper(II) ion via two oxygen and one nitrogen atoms. The characteristic ν(N−H), ν(C=O), ν(C=N) and ν(N− N) bands appeared at 3257, 1593, 1563 and 1090 cm^{-1} in the complex. The IR spectrum of the ligand shows absorption bands of ν(N−H), ν(C=O), ν(C=N) and ν(N−N) at 3253, 1580, 1603 and 1103 cm^{-1}. From the perusal of complex and ligand IR absorption bands, it is clear that ν(N− H) remains unshifted, which shows that NH is not deprotonated upon complexation. The absorption band of the C=O is downward shifted in the metal complex. Therefore, carbonyl oxygen is coordinated with metal ions as confirmed by the X-ray structure. The absorption band of C=N is also downward shifted and therefore, it is reasonable to consider that azo nitrogen (>C=N) is coordinated to the metal. The band due to ν(N−N) is seen in both HL and metal complex but upshifted in metal complex, suggesting coordination of the nitrogen atom of >N−N< group to the metal (Fig. 9 and 10). In metal complex new bands at 1450, 1388 and 1031 cm^{-1} displayed are due to a coordinated nitrate ion. The coordinated unidentate nitrate displayed these bands owing to the $\nu_{asym}(NO_2)$, $\nu_{sym}(NO_2)$ and ν(NO) vibrating modes. One non-ligand band seen at 436 cm^{-1} corresponds to ν(M−O) stretching vibration.

Electronic spectral studies

The ligand field absorption spectrum is also measured. The visible absorption spectra is observed by the intense bands at a shorter wavelength. The band originates at 614 nm has $^2T_2 \rightarrow {}^2E$ transition. The most striking spectroscopic feature is the appearance of a band at 408 nm due to ligand to metal charge-transfer (LMCT) transition. One more high-energy intense band observed at 303 nm is due to the $\pi\cdots\pi^*$ transition of the Schiff base. Such spectral features have already been discussed in several pseudo-tetrahedral copper(II) complexes.

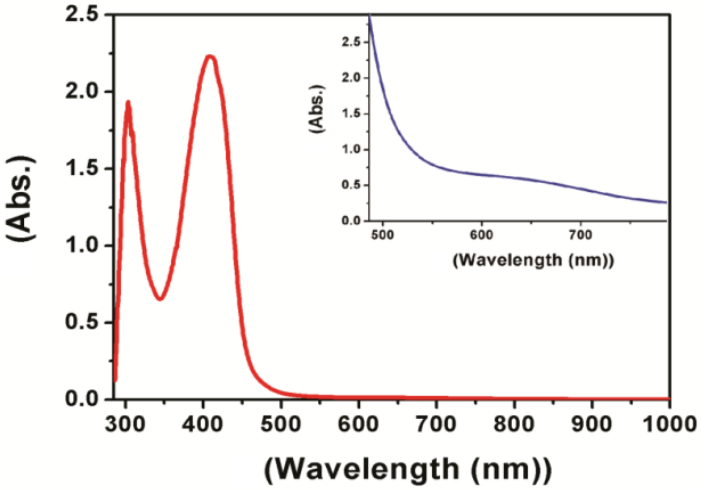

Absorption spectra of 1×10^{-3} M DMSO solution of the complex **[Cu(L)(NO_3)]**.

Electrochemical studies

The redox properties of this complex were investigated in DMSO (0.003 mL^{-1}) using cyclic voltammetry. Tetra butyl ammonium perchlorate (TBAP) was used as a supporting electrolyte. Cyclic voltammograms were recorded with 100 and 200 mVs^{-1} scan rates vs Ag/AgCl as the reference electrode.

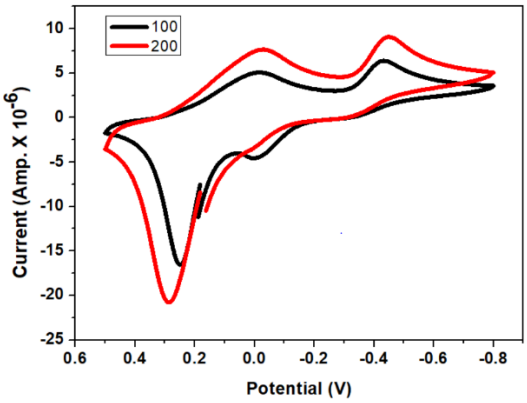

Cyclic voltammogram of the complex **[Cu(L)(NO_3)]** in DMSO.

Epr spectral study

Epr spectra of complex recorded in polycrystalline at room temperature and in DMSO solution at liquid nitrogen temperature (LNT). The polycrystalline spectrum (RT) exhibited a broad absorption at <g> = 2 . The frozen DMSO solution epr spectrum showed the typical four-line patterns expected for coupling of the electron to the 3/2 spin of a copper nucleus. The hyperfine coupling constant ($A_{\parallel}$ = 175 × 10^{-4} cm^{-1}) and g-value ($g_{\parallel}$ = 2.228, $g_{\perp}$ = 2.075) are very close to those found for similar pseudo-tetrahedral copper(II) complexes.

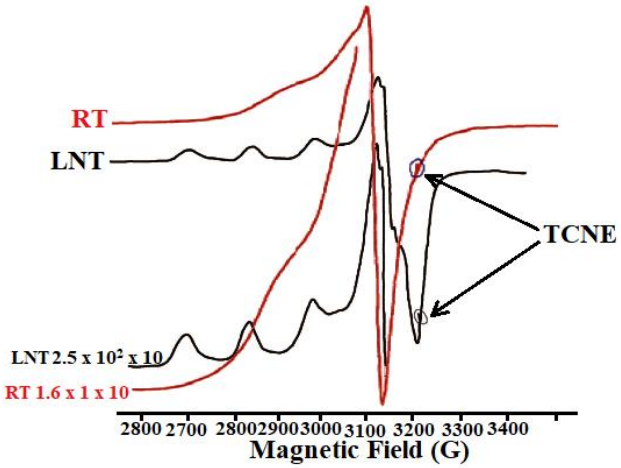

Epr spectrum of the complex **[Cu(L)(NO$_3$)].**

ESI-Mass

ESI-Mass analyses of complexes were performed.

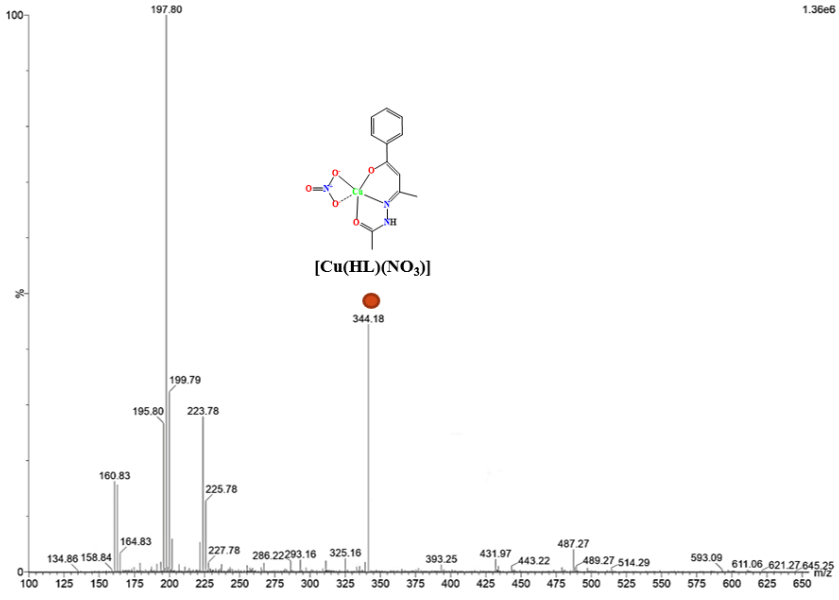

The ESI-Mass spectrum of the complex **[Cu(L)(NO$_3$)].**

Antioxidant superoxide dismutase

The *in vitro* antioxidant superoxide dismutase mimetic activity of this complex was measured using the alkaline DMSO-nitroblue tetrazolium (NBT) assay system. A plot of percent inhibition of NBT versus concentration of complex. The concentration (µM) equivalent to the unit of SOD activity (IC_{50} value) 16 μM. As the reaction proceeds, the reduction of NBT to MF^+ was measured at 560 nm. The estimated IC_{50} value of the present complex is compared with the IC_{50} value of similar mononuclear complexes reported in the literature.

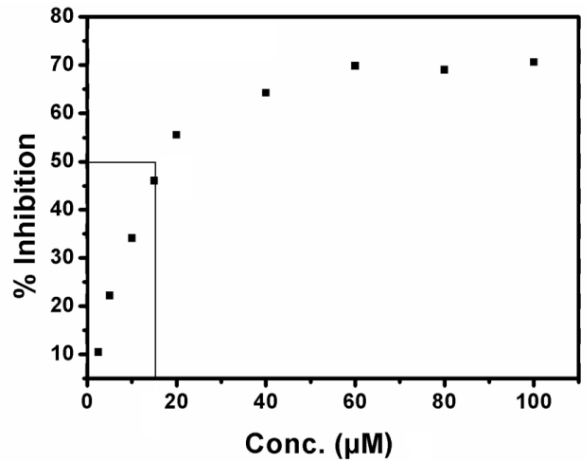

A plot of % inhibition of NBT reduction vs concentration of complex **[Cu(L)(NO$_3$)]**.

Anti-cancer activity of complex

Anticancerous potential of the synthesized complex was evaluated using cytotoxicity assay. The complex showed considerable cytotoxic activity. After treatment of 24 hours, inhibition concentration 50 (IC_{50}) value was calculated using probit analysis against positive standard Cisplatin. THE derived IC_{50} value was shown in Fig. 16. Comparative effects of treatments *vs* cisplatin on various cell lines are given in Table 5. The complex was efficacious than cisplatin in its effect. HepG2 has shown effective percent inhibition 21.88±1.3µM) among other cell lines used for the study.

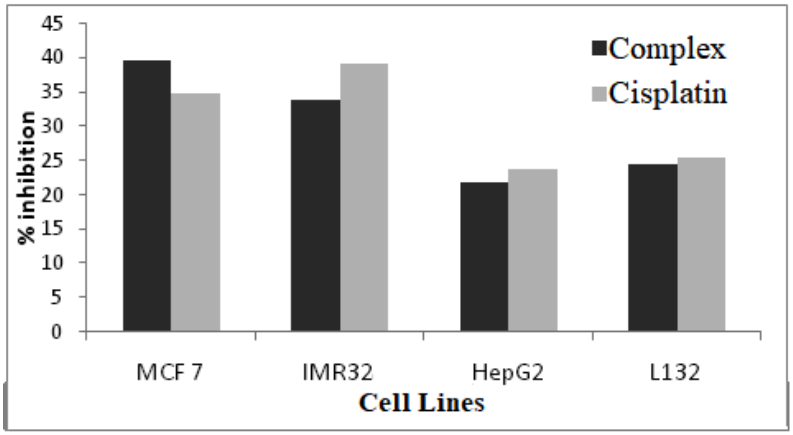

Showing % inhibition (µM) of cells of various cell lines after 24 hours of synthesized compound treatment.

Cells were treated by complex for 24 hours to observe cell death. Cells were stained by acredine orange (AO) and ethidium bromide (EB). Cells were stained by AO were live cells whereas stained by EB were necrotic cells but apoptotic cells were stained by AO and EB both.

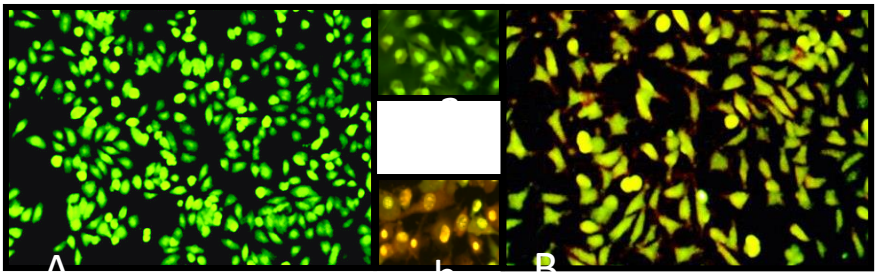

Showing dual staining of HepG2 cells A) Untreated cells stained by acredine orange (Viable cells), cytoplasm and nucleus emitted green (a) fluorescence, B) Treated cells stained by acredine orange and ethidium bromide both, Inset picture (b) with apoptotic characteristic.

HepG2 cells were treated by complex for 12 and 24 hours and fold change in expression was calculated. The level of Bax has observed fold increased after treatment of compound whereas expression of Bcl2 was down-regulated (Fig. 16). Furthermore, expression of p53 and caspase 9 were also fold elevated due to treatment of copper complex. Similar anti-proliferative properties were studied on copper(II) complex.

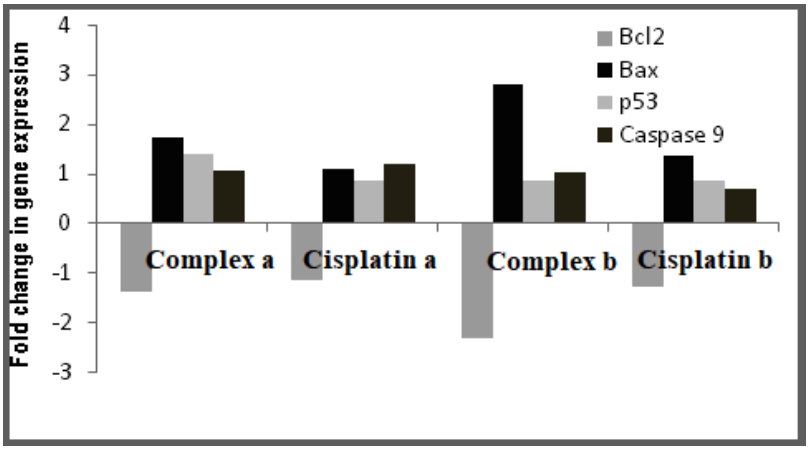

Gene expression study after 12- and 24-hours exposure of selected compound on HepG2 cell line (a: 12 hours; b: 24 hours).

Conclusions

The new mononuclear complex ($Cu(HL)NO_3$) where HL = (N'-[(2E,3Z)-4-hydroxy-4-phenylbut-3-en-2-ylidene]acetohydraziede) was obtained. The Schiff base coordinates through metal ion via two nitrogen and one oxygen atoms. Hence Schiff base behaves as a tridentate ligand. The crystallographic data reveal that the metal ion is also coordinated to nitrate ligand forming pseudo-tetrahedral geometry. Such geometry around copper(II) is very less common. We have also characterized complex by various spectroscopic techniques. Spectroscopic features consistence of UV-Vis, IR, CV, Epr, Hirshfeld and XRD data with DFT calculations of four coordinated copper(II) complex used to understand the electronic structure of this pseudotetrahedral complex. The results obtained from DFT calculations have been compared with the experiment and showed good agreement. This complex showed good antioxidant SOD properties. The complex also exhibits good anticancer activity prominent anticancer properties *in vitro*. The antiproliferative properties of this complex have opened the avenues to design and synthesize new members of the same ligand framework to investigate a better anticancer drug.

Chapter 3

Copper(II) complexes incorporating NNN-tridentate hydrzone as proligand

(A) Synthesis and structural characterization of Copper(II) complexes with flexible hydrazone: Structural diversity, Hirshfeld analysis, density functional calculations and biological study

The reaction of Schiff base ligand HL = (Z)-2-(phenyl(2-(pyridin-2-yl)hydrazono)methyl)pyridine condensation of 2-hydrazino pyridine and 2-benzoyl pyridine with either $CuCl_2.2H_2O$ and $Cu(SO_4).5H_2O$ in a 1:1 molar ratio yields $[Cu(Cl)_2(L)]$ **1** and $[Cu_2(\mu\text{-}SO_4)_2(L)_2]$ **2**, in which the NH group of HL remains deprotonated (Table 1). The synthetic routes used for the synthesis of **1** and **2** are depicted in Scheme 2. These complexes were synthesized in good yield. Both complexes **1** and **2** are air-stable. All general characterizations were carried out with crystalline samples. Microanalyses showed that the components of both complexes are well consistent with the results of molecular structural analysis. Single crystal X-ray analysis showed that complex **1** is mononuclear whereas **2** is the binuclear complex.

Experimental
Synthesis of Ligand HL

Schiff base ligand HL = (Z)-2-(phenyl(2-(pyridin-2-yl)hydrazono)methyl)pyridine was synthesized by taking 2-hydrazinopyridine (1.091g, 10 mmol) in absolute ethanol (50 mL) and 2-benzoyl pyridine (0.78g, 10 mmol) was added with few drops of glacial acetic acid as a catalyst. The synthesis of a ligand is shown in Scheme 1. The resultant mixture was stirred at room temperature for 30 min and then refluxed at 75°C for 3 hrs. The yellowish solution was filtered and the filtrate was kept for slow evaporation at room temperature to yield a light-yellow polycrystalline sample. The Schiff base was washed with ethanol and dried over fused $CaCl_2$. Yield: 75 %. Anal. Calc. for $C_{17}H_{14}N_4$ (274.33 g mol^{-1}): C, 74.52; H, 5.54; N, 20.04 %. Found: C, 74.55; H, 5.51; N, 20.06 %. FTIR (KBr, cm^{-1}): 1592 ν(C=N). ^{1}H NMR (DMSO-d_6 400 MHz) δ: 12.9 (s, 1H, -NH-), 8.8 (d, 2H, CH=N) 8.0-7.2 (t, 3H, CH benzylidenimin), 8.8–7.8 (m, 8H, CH 2-pyridiene) ppm. ^{13}C NMR (DMSO-d_6 400 MHz) δ: 156 (CH=N-), 152 (Ar-CH=N), 152 (C-NH-), 149-105 (Ar-C) ppm.

Synthesis of Complex $[Cu(Cl)_2(L)]$ 1

The Schiff base ligand (0.274g, 1.0 mmol) was dissolved in methanol (20 mL). A solution of $CuCl_2.2H_2O$ (0.134 g, 1.0 mmol) in methanol (20 mL) was added dropwise to the above solution with stirring for 5 hrs to give a green colour solution. The resulting solution was filtered. The filtrate was left for slow evaporation at room temperature. Plate-like crystals were formed from the solution two weeks later. These crystals were washed with hot distilled water and then ethanol to remove impurities. The crystals were dried under a vacuum. Yield: 80 %. Anal. Calc. for $C_{17}H_{15}Cl_2CuN_4$ (408.77 g mol^{-1}): C, 49.80; H, 3.65; N, 13.61 %. Found: C, 49.83; H, 3.69; N, 13.60 %. FTIR (KBr, cm^{-1}): 1564 ν(C=N), 417 (s) ν(Cu–N).

Synthesis of Complex $[Cu_2(\mu\text{-}SO_4)_2(L)_2]$ 2

The Schiff base ligand (0.274 g, 1.0 mmol) was dissolved in methanol (20 mL). A solution of $CuSO_4.5H_2O$ (0.159 g, 1.0 mmol) in methanol (20 mL) was added dropwise to the above solution with stirring for 5 hrs to give a green clear solution. The resulting solution was filtered. The filtrate was left for slow evaporation at room temperature. Plate-like crystals were formed from the solution two weeks later. These crystals were washed with hot distilled water and then ethanol to remove impurities. The crystals were dried under a vacuum.
Yield: 80 %. Anal. Calc. for $C_{68}H_{80}Cu_4N_{16}O_{28}S_4$ (1951.88 g mol^{-1}): C, 46.82; H, 3.75; N, 12.35 %. Found: C, 46.84; H, 3.72; N, 12.32. FTIR (KBr, cm^{-1}): 1568 ν(C=N), 462(s) ν(Cu-O), 417(s) ν(Cu–N).

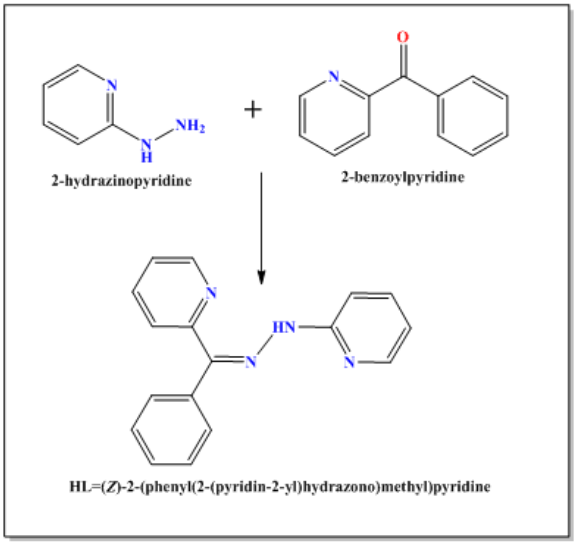

Scheme 1 Synthetic route of Ligand (**HL**).

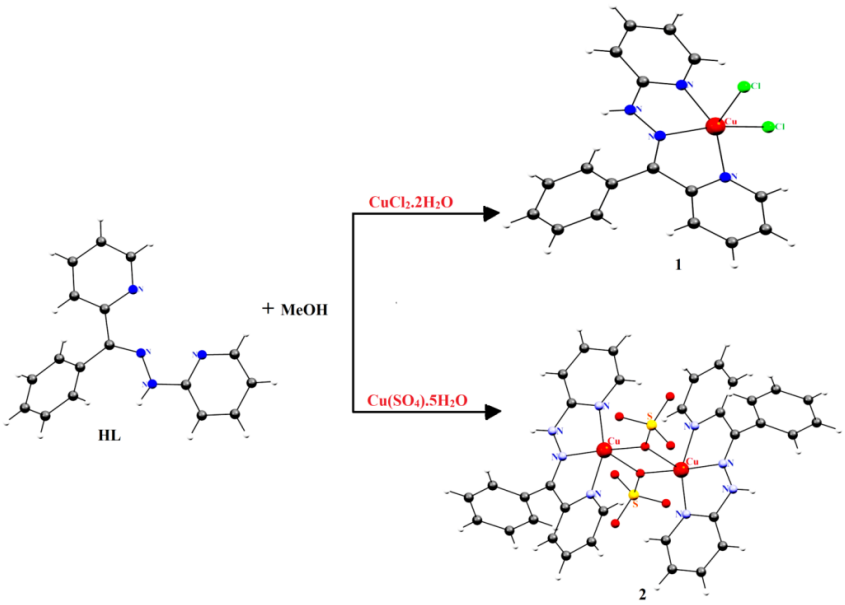

Scheme 2 Synthetic route of metal complexes **1** and **2.**

FTIR analysis

In the FTIR spectrum of complex **1**, peaks at 3433 and 1459 cm^{-1} are characteristic peaks that are assigned for N-H stretching and bending modes respectively. Similarly, for complex **2**, peaks at 3406 and 1464 cm^{-1} are observed. The sharp $> C = N$, stretching vibration bands corresponding to the imine group of Schiff base framework appear at 1568 cm^{-1} and Skelton vibrations of phenyl groups at 1480 and 1542 cm^{-1}. The redshifts in the vibrational absorption bands of $> C = N$ the group composed of 1592 cm^{-1} of free Schiff base agree with the coordination of Schiff base to the copper(II) center. The observed vibrational bands at 427 and 462 cm^{-1} are due to ν(M-N) and ν(M-O) stretching frequencies in complex **2**. Other bands associated with the Schiff base showed minor shifts, suggesting that the electron density of the bonds has been altered on coordination.

Molecular structure of HL and complexes

Both pyridine rings remain in the plane while phenyl rings out off plane. The bond length in between C1 and N3 azomethine nitrogen (>C=N) is smaller compared to C7 and N2 protonated imino nitrogen. The smaller bond length is due to the presence of a double bond in between C1 and N3 (azomethine nitrogen).

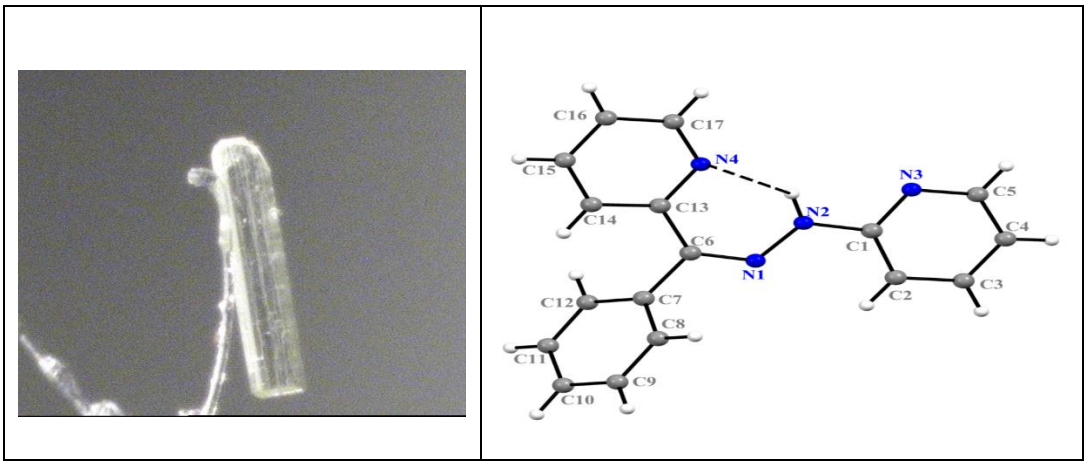

The ORTEP diagram of **HL** with crystal image.

The Molecular structures of complex **1** are shown in Fig. 10-13 respectively. Complex **1** is mononuclear, whereas **2** is the binuclear complex. In both complexes, Schiff base ligand acts tridentate *via* NNN donor atom set and is mono diprotonated (L^-). The binuclear co-crystal of complex **2** has a non-centrosymmetric structure with a binuclear $Cu_2(Cu\text{-}O\text{-}R)_2$ rectangular core. One oxygen atoms of sulfate anion act as a bridge between two copper(II) metal centers. The coordination geometry around each copper(II) center is distorted pyramidal. The relative amounts of the distorted square pyramidal are given by an Addition's factor (τ_5). The τ_5 values for two copper(II) centers are estimated as $(\tau_5)_1$ = 0.3 and $(\tau_5)_2$ = 0.2. Thus, the coordination environment of each copper(II) is a slightly distorted square pyramidal structure in which four equatorial sites comprised of O(1A), N(3A), N(1A) and N(A) with the axial position occupied by one of the oxygen atoms of sulphate anion coordinated to the second copper(II) center, acting as bridging ligand.

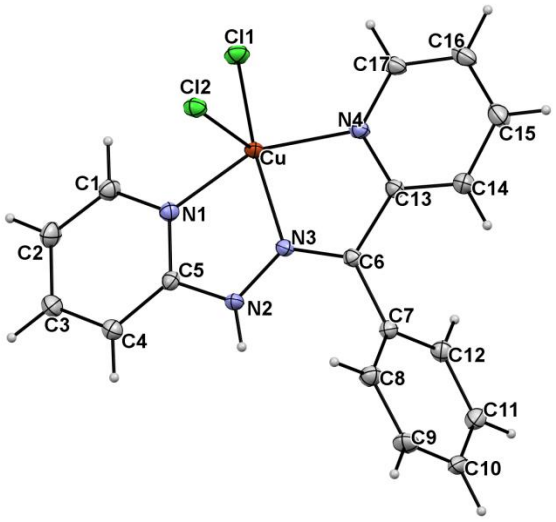

Molecular structure of complex **1**.

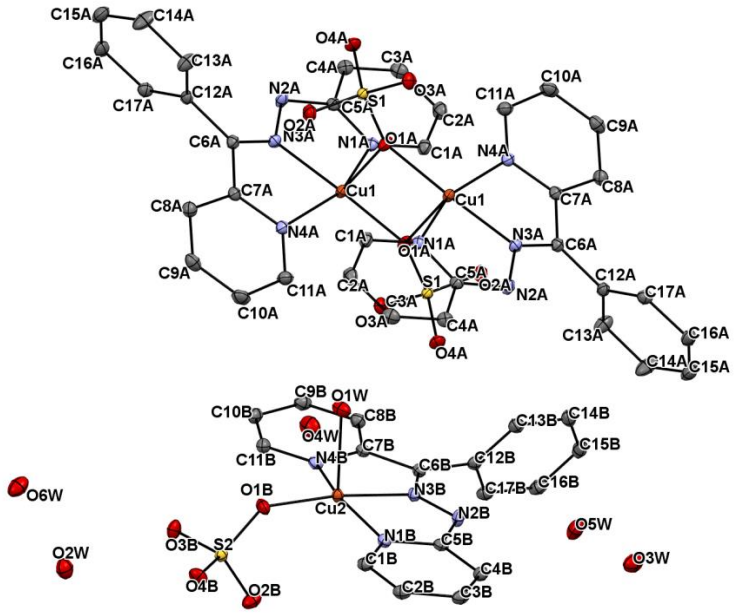

Molecular structure of complex **2.**

Electrochemical studies

The electrochemical behaviours of both complexes was studied using cyclic voltammetry (CV) and differential pulse voltammetry (DPV) techniques. Both complexes display two reduction peaks at +0.21 V ($Cu^{2+} \rightarrow Cu^{+1}$) and -0.34 V ($Cu^{+} \rightarrow Cu^{0}$) and one oxidation peak at -0.28 V($Cu^{0} \rightarrow Cu^{2+}$) of **1** and reduction peaks at -0.20 and -0.27 along with oxidation peak at -0.15 V ($Cu^{0} \rightarrow Cu^{2+}$) for **2,** respectively**.** This may be due to the chemical oxidation of copper during the complexation processes i.e. during complexation processes the Cu^{+1} species is transformed to Cu^{2+} and ligand is reduced at a more negative potential on increasing the scan rate peak currents increases linearly, supporting the diffusion effect on the electrochemical (E_c) mechanism.

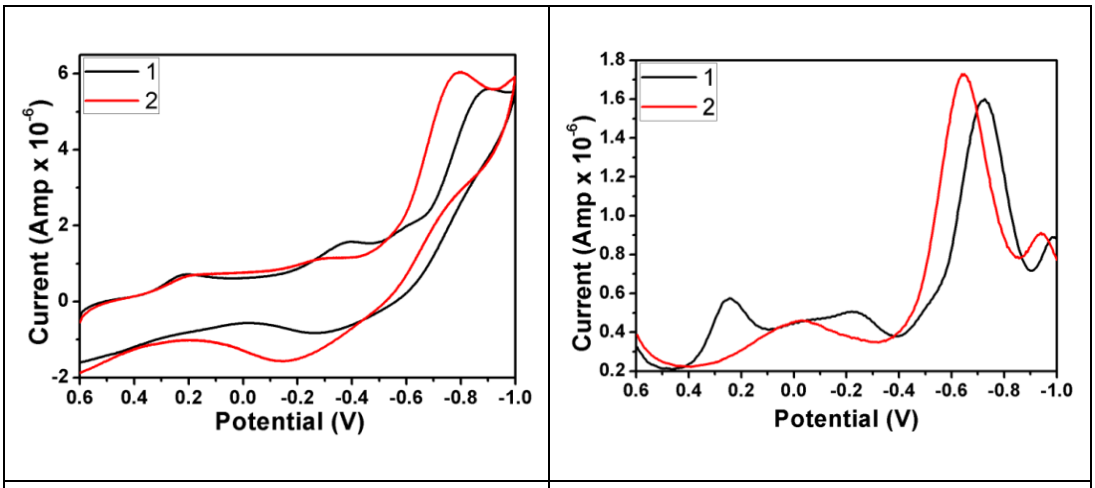

(a) Cyclic voltammograms of complexes 1and 2 in DMSO at an Ag/AgCl electrode with a scan rate of 300 mV s^{-1} and temperature 20°C. (b) Differential pulse voltammogram of complexes **1** and **2** at room temperature using a scan rate of 20 mV s^{-1}in DMSO. The pulse amplitude is 50 mV.

EPR measurements

The Epr spectra of complexes **1** and **2** were measured in a Varian E-line Spectrometer working in the X-band at RT of polycrystalline and LNT of frozen solutions. The Epr spectra of these complexes were recorded in polycrystalline samples at RT and in DMSO solution (3×10^{-3} M) at LNT.

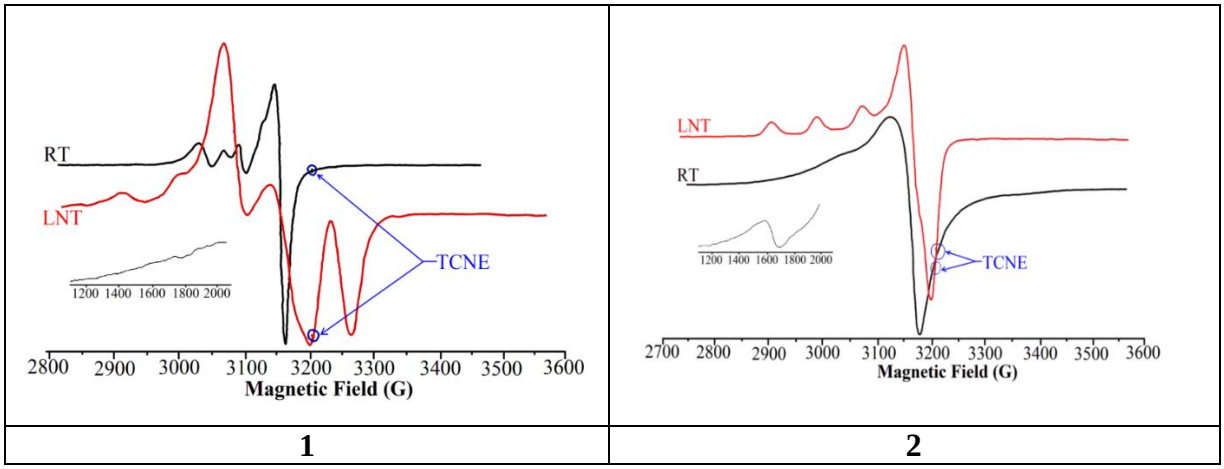

X-band EPR spectra of complex 1 and 2 in the polycrystalline state (RT) and DMSO solution at LNT. Inset: EPR spectra showing half-field signals.

Cryomagnetic susceptibility studies

The thermal variation $\chi_M T$ (χ_M = molar magnetic susceptibility) for **1** and **2** in the temperature range 300-2 K. The value of the $\chi_M T$ product obtainedat room temperature for complex **1** is 0.43 cm^3 $Kmol^{-1}$, which is slightly larger than the value expected for an isolated S = ½ copper(II) ion (0.375 cm^3 K mol^{-1}). On cooling, the $\chi_M T$ product remains roughly constant until approximately 45 K when a slight decrease in thisvalue is observed. Further cooling of the sample leads to a sharper decrease in $\chi_M T$ which is ascribed to antiferromagnetic interactions.

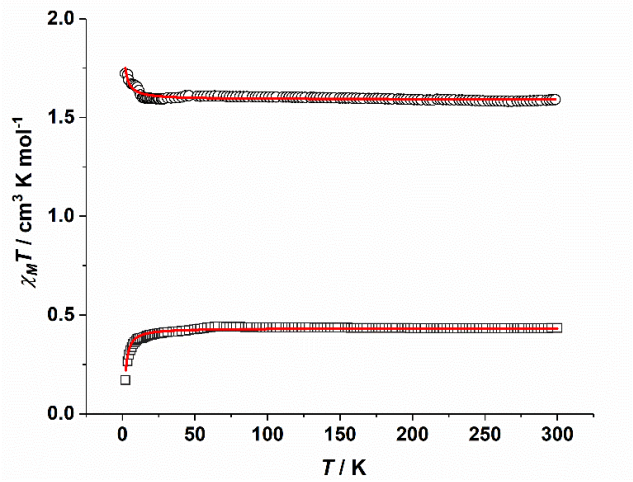

Temperature dependence of the *product* $\chi_M T$ of complexes **1** (squares) and **2** (circles) measured under a magnetic field of 0.5 T. The solid lines represent the fit of the data as described in the text.

DFT calculations

To help the physicochemical data (Epr and CV) DFT calculations were executed on complexes **1** and **2**. Geometry optimization was performed using density functional theory (DFT) at the B3LYP basic set. The analysis of the frontier molecular orbital of the optimized structures shows that, in the gas phase, the highest occupied molecular orbitals (HOMOs) and lowest occupied orbitals (LUMOs) of both complexes are similar in energy. It is observed that the HOMOs of both complexes were mainly ligand centered, with the major contributions due to the *p* orbitals of donor atoms.

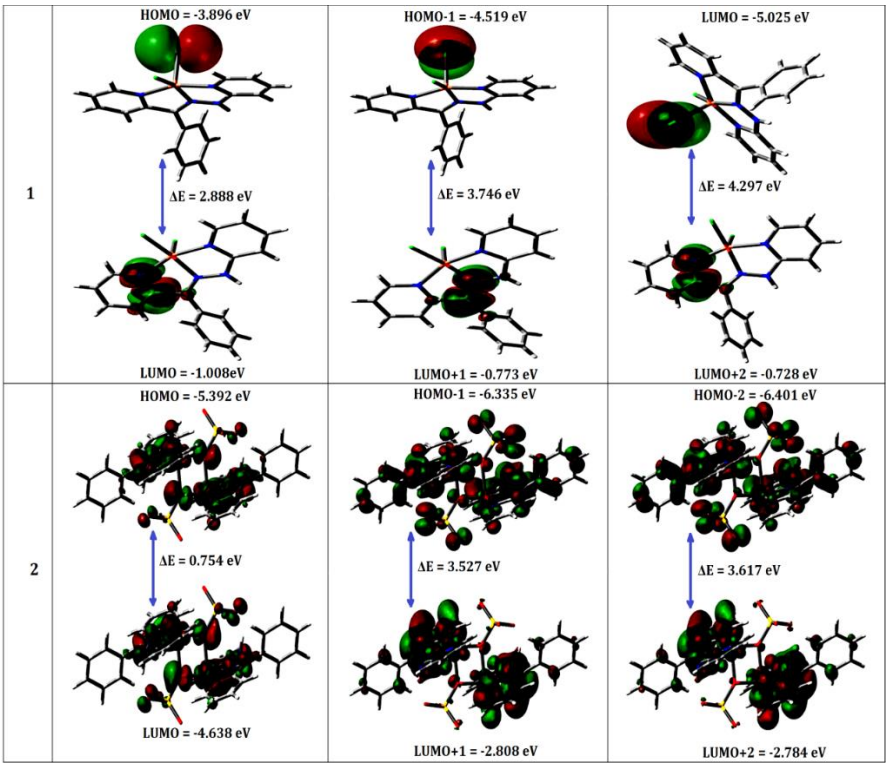

HOMO-LUMO structures with energy level diagrams of complex **1** and **2**.

Hirshfeld Surface Analysis of HL and complexes

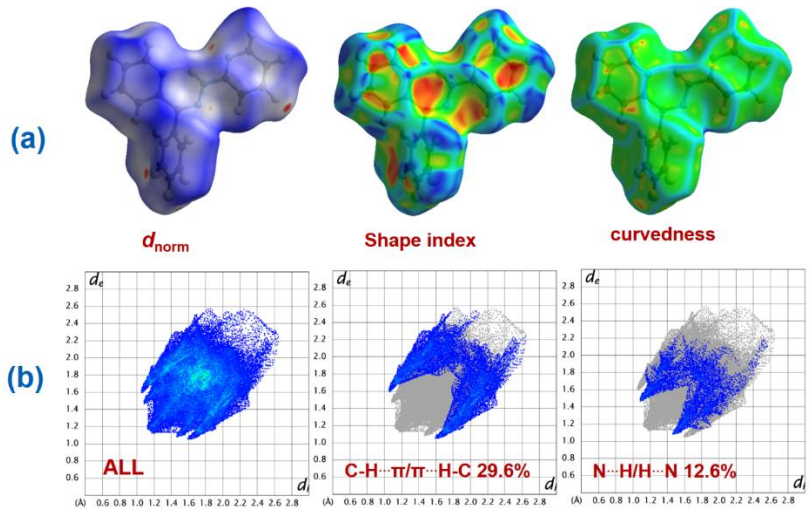

Hirshfeld surfaces mapped with d_{norm}, shape index and curvedness for the ligand; (b). Fingerprint plots for the ligand showing percentages of contact contributed to the total Hirshfeld surface area of the ligand molecule.

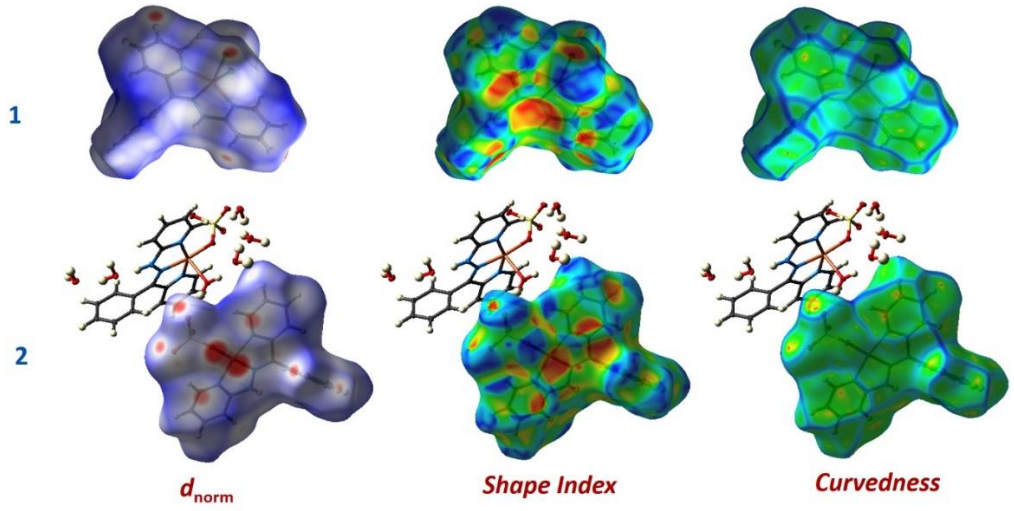

Hirshfeld surfaces mapped with d_{norm}, shape index and curvedness for the complexes **1** and **2**.

Reactivity with superoxide

Superoxide anion ($O_2^{\cdot-}$) is often employed to get information on M - $O_2^{\cdot-}$ interactions. The *in vitro* antioxidant superoxide reactivity of complexes has been evaluated using the alkaline DMSO-nitro blue tetrazolium (NBT) method.

SOD activities (IC_{50} values kinetic catalytic constant and SOD activity) of Cu(II) complexes.

S. No.	Complex	IC_{50} (μM)	SOD activity (μM^{-1})	k_{cat} ($M^{-1}S^{-1}$)	Reference
1.	Vc	852	1.17	0.39	60, 61
2.	$[Cu(L)Cl_2]$	15	66.67	22.18	Present work
3.	$[Cu_2(\mu\text{-}SO_4)(L)_2]$	22	45.45	15.12	Present work

Cytotoxicity Assay

The anticancer activity of complexes **1**, **2** and ligand (**HL**) was assessed against four types of cancer cell lines IMR 32 (neuroblastoma), MCF 7 (breast cancer), HepG2 (hepatocellular carcinoma) and A549 (lung cells) have been examined in comparison with the positive standard cisplatin under identical conditions by using MTT assay.

The *in vitro* cytotoxic activity (expressed as IC_{50}) of copper complexes against the different cell lines.

Compound	IC_{50} Value(μM)			
	MCF 7	IMR 32	HepG2	A549
1	105.6236	112.6543	101.209	119.194
2	184.2575	207.68	168.6424	174.107
Ligand	84.27725	87.56933	79.88781	75.169
Cisplatin	34.59	38.99	31.04	25.33

Conclusions

Two new mono and binuclear copper(II) complexes were synthesized by a biomimetic strategy and their structures were solved by single-crystal X-ray and various spectral techniques. All the copper centers in both complexes have pentacoordinate geometries. This kind of geometry has been observed also some known di- or polynuclear copper(II) complexes. Low-temperature susceptibility measurements revealed that the copper(II) centers in both complexes **1** and **2** are weakly anti-ferromagnetically coupled. Complex **2** is a unique example showing Ferro- and antiferromagnetic couplings. The ferromagnetic coupling in the two symmetric sulphate bridges fully agrees with the previous magneto-structural correlations. Antioxidant SOD activities were also examined. Both complexes are potent SOD mimics. The structures-activity relationship for complexes was studied to support the experimental findings to assess some important parameters, *viz.*, bond length, bond angle, HOMO-LUMO energy gap (ΔE), global reactivity descriptors, dipole moment, second-order perturbation energies and spin density. The antioxidant SOD and antiproliferative properties *in vitro* suggest the encouraging applications of **1** and **2** in biology and pharmaceuticals sciences.

Chapter: 3

(B) Penta-coordinated copper(II) complexes with hydrazido based ligand and imidazole as auxiliary ligand: Synthesis, spectral characterization and SOD mimetic activities

The high therapeutic features of the imidazole related drugs have promoted the medicinal chemists to synthesize a large number of chemotherapeutics compounds. The molecular formulations of these complexes are as $[Cu(L)(ImH)_2](ClO_4)_2$ **(1)**, $[Cu(L)(2\text{-}MeImH)_2](ClO_4)_2$ **(2)**, $[Cu(L)(2\text{-}EthImH)_2](ClO_4)_2$ **(3)**, $[Cu(L)(BenzImH)_2](ClO_4)_2$ **(4)** and $[Cu(L)(2\text{-}MeBenzImH)_2](ClO_4)_2$ **(5)** (Where ImH = Imidazole, 2-MeImH = 2-Methylimidazole, 2-EthImH = 2-Ethylimidazole, BenzImH = Benzimidazole, 2-MeBenzImH = 2-Methylbenzimidazole**)**. The spectral and electrochemical behaviour of these complexes were also studied. The magnetic properties of these complexes are similar from those of previously reported mononuclear copper(II) complexes with Schiff bases and co-ligands. Additionally, in this chapter SOD mimetic activities have been examined and compared with known SOD mimics.

Synthesis of complex $[Cu(L)(ImH)_2](ClO_4)_2$ 1

To a methanolic solution (10 mL) of $Cu(ClO_4)_2.6H_2O$ (0.370 g, 1 mmol) HL (0.274 g, 1 mmol) was added while stirring. A methanolic solution (10 mL) of imidazole (0.136 g, 2 mmol) was added to the above solution drop-wise and resulting reaction mixture gradually changed to green colour. After 1 hrs of stirring the microcrystalline solid was filtered and washed with ethanol. This microcrystalline powder was isolated and dried in $CaCl_2$ desiccator. Yield: 81 %. Anal. Calc. for $C_{23}H_{22}Cl_2CuN_8O_8$ (672.92 g mol^{-1}): C, 41.05; H, 3.30; N, 16.66 %. Found: C, 41.07; H, 3.32; N, 16.64 %. FTIR bands (KBr, cm^{-1}): 1537 ν(C=N),1086 ν(N–N). m/z: 672.02.

Similarly, all other complexes were synthesized.

Results and discussions

The reaction of $Cu(ClO_4)_2.6H_2O$ with hydrazone and co-ligands led to the formation of mononuclear **1-5** complexes. These complexes were isolated in good yield and characterized using UV-vis, FTIR and epr spectral physico-cemical techniques. The all complexes are insoluble in water and non-polar organic solvents but are highly soluble in DMSO and CH_3CN. These complexes are stable in air.

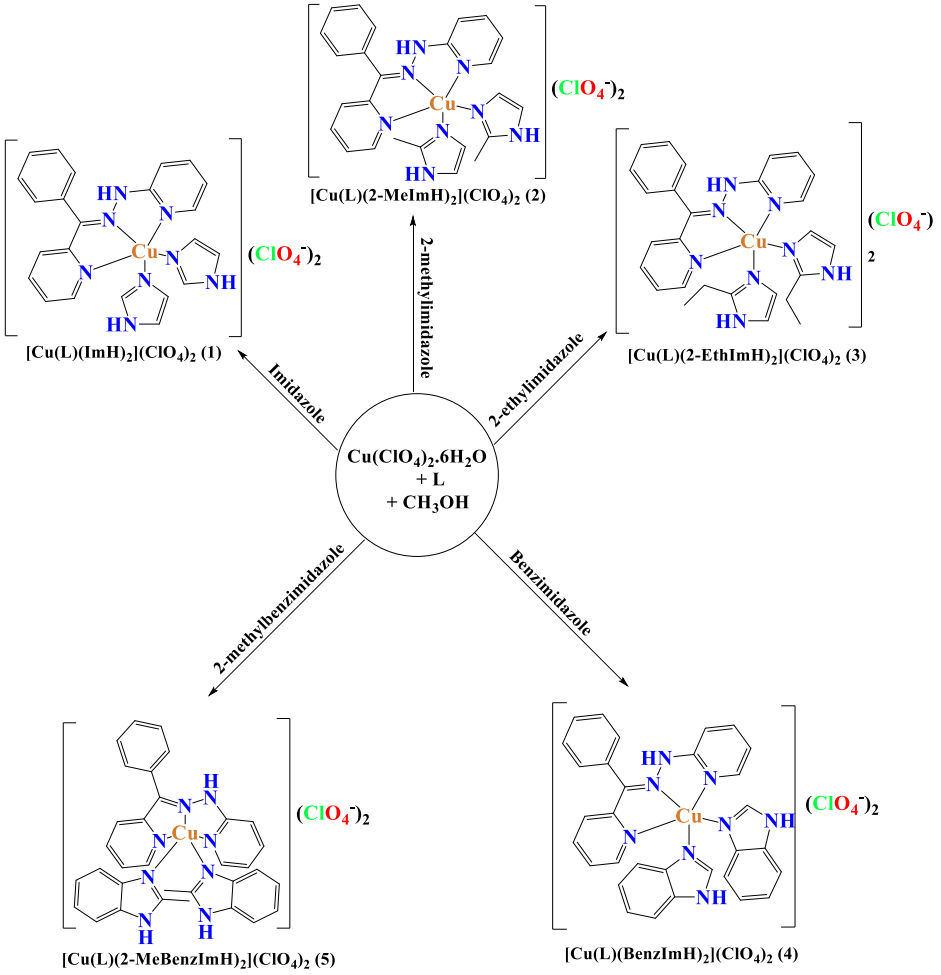

Scheme 1 General synthetic route of complexes **1-5**.

FTIR spectra

FTIR spectral band assignments of L and complexes.

Compounds	ν(NH)	ν(>C=N)	ν(N-N)	ν(Cu-O)	ν(Cu-N)
L	3084	1592	988	-	-
1	3420	1537	1086	486	423
2	3396	1569	1020	461	421
3	3417	1572	1093	461	419
4	3421	1563	1018	418	411
5	3421	1563	1018	419	411

Electronic spectra

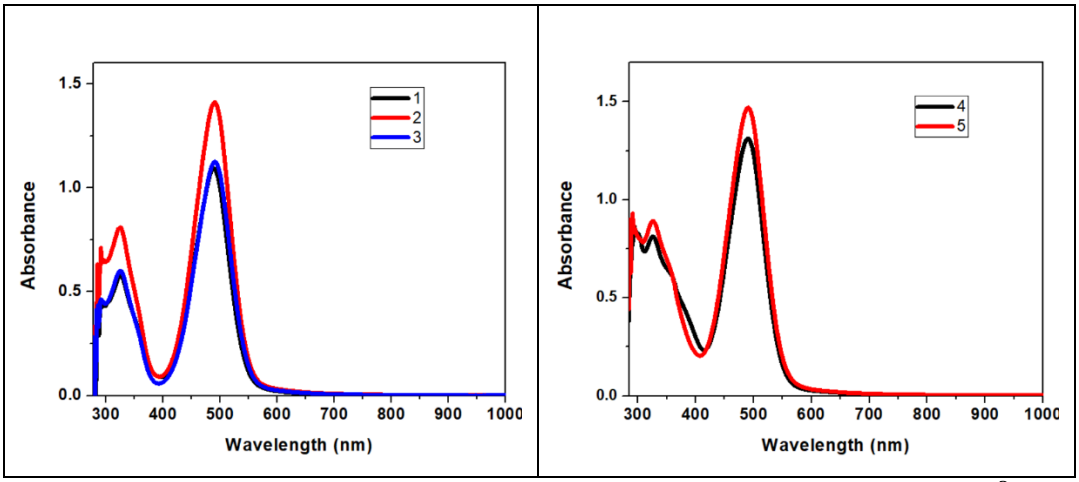

UV-visible spectra of copper(II) complexes **1-5** in DMSO solution 1.0 x 10^{-3} M.

Epr Study

Epr parameters of copper(II) complexes in polycrystalline state at 298K and in DMSO solution at 77K.

Complex	RT (Polycrystalline)				LNT (Solution) in DMSO (77K)		
	$g_{\parallel}$	$g_{\perp}$	G	D(cm^{-1})	$g_{\parallel}$	$g_{\perp}$	$A_{\parallel}$(G)
1	g_{iso} = 2.084		-	0.018	2.182	2.047	177
2	2.264	2.070	3.866	0.055	2.177	2.048	187
3	2.263	2.069	3.910	0.056	2.177	2.050	175
4	2.237	2.057	4.290	0.052	2.197	2.047	170
5	2.211	2.053	4.110	0.052	2.222	2.049	177

Theoretical studies

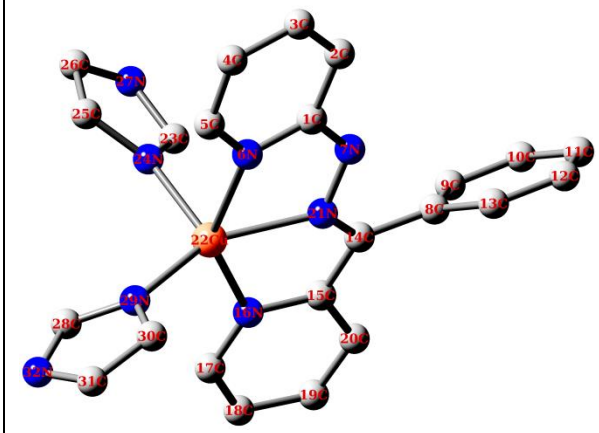

1

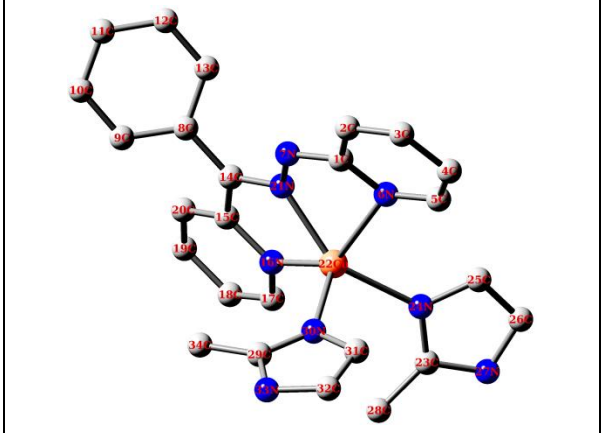

2

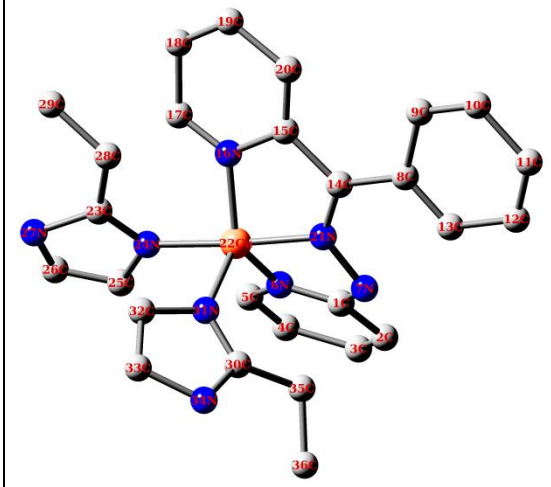

3

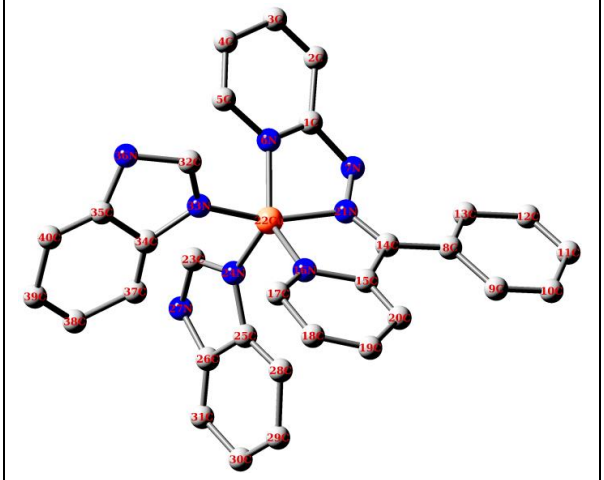

4

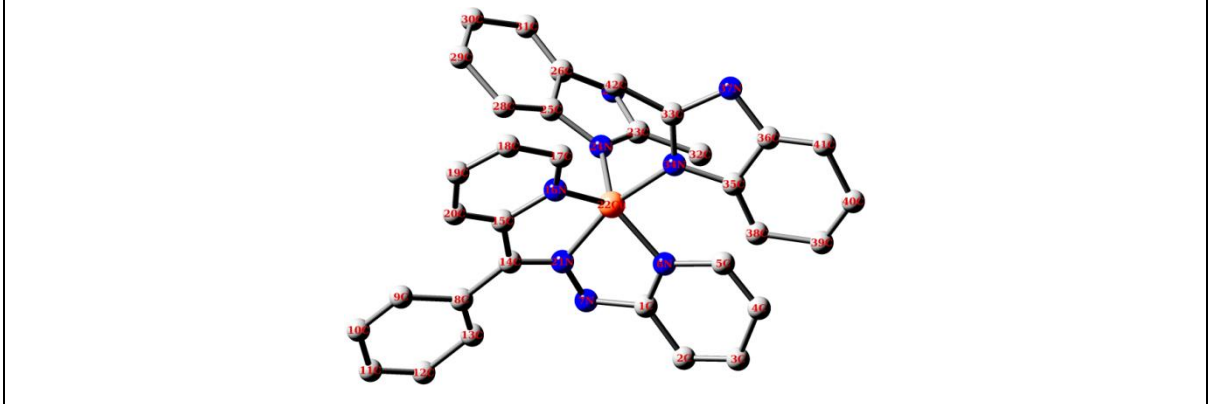

5

Optimized structure of complexes **1-5**.

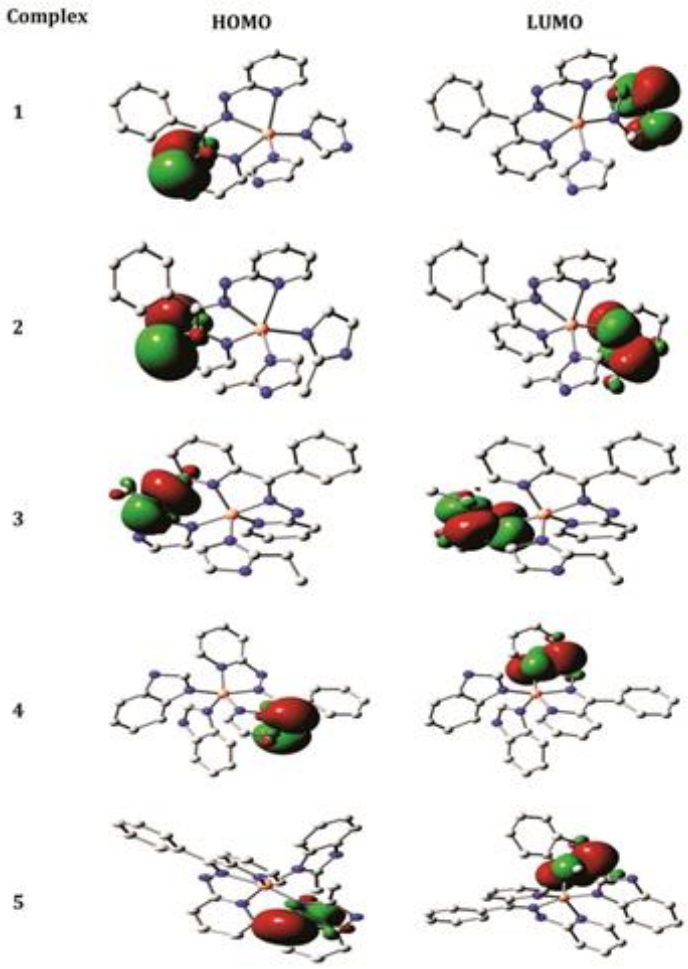

Presentation of frontier molecular orbitals of complexes **1-5**.

SOD activity

The antioxidant SOD activity IC_{50} and kinetic catalytic constant for complexes **1-5**.

Compound	IC_{50} (μM)	SOD activity (μmol^{-1})	k_{M_cCF} $(molL)^{-1}s^{-1} \times 10^4$	References
[Cu(BHM)ImH].CH_3OH	27	37.03	12.32	72
[Cu(BHM)(bipy)]	62	16.62	5.36	72
[Cu(L)$(NO_3)_2$(4,4-bipy)]	30	33.33	11.08	58
[Cu(L^1)(HL^1)]ClO_4.1/2H2O	25	40.00	13.30	58
[Cu(HL^2)$(H_2O)_2]_2NO_2$	16	62.50	20.79	73
Vc	852	1.17	0.39	74
1	26	38.46	12.79	Present work
2	43	23.25	7.73	Present work
3	41	24.39	8.11	Present work
4	39	25.64	8.53	Present work
5	35	28.57	9.50	Present work

Conclusions

In this chapter we have synthesized five copper complexes using $Cu(ClO_4)_2.6H_2O$ and hydrazone ligand (HL) with using different imidazole series as co-ligand led to the formation of mononuclear complexes. These complexes were isolated in good yield and characterized using UV-Vis, FTIR and EPR spectral physico-chemical techniques. The all complexes are insoluble in water and non-polar organic solvents but are highly soluble in DMSO and CH_3CN. These complexes are stable in air. The molar conductance value of complexes are in the range 118-139 (Ω^{-1} cm^2 mol^{-1}) in DMSO solution. The room temperature magnetic susceptibility data of all complexes collected. The room temperature magnetic moment values are in the range 1.79-1.81 B.M. The magnetic moment values are very close to the spin only value for the discrete magnetically non-coupled copper(II) system, suggesting that the complexes are non-coupled at room temperature. The copper(II) centre in all complexes are penta-coordinated. The proligand has NNN donor sites viz., two pyridine N and one azomethine N atoms whereas co-ligand coordinates through pyridine N atom forming two five membered chelate rings. Both pro and co-ligands are neutral. Thus geometry around copper(II) ion remain square pyramidal. The τ_5 values of theses complexes are in the range 0.177-0.495. The IC_{50} value of present complexes remains in the range 26-43 µM.

Chapter: 3

(C) Synthesis, spectral characterization and biomimetic activity of homobinuclearcopper(II) 2-[(E)-phenyl(pyridine-2-yl-hydrazone)methyl]pyridine complexes containing inorganic salts

In this part of thesis, homo binuclear copper(II) 2-[(E)-phenyl(pyridine-2-yl-hydrazono)methyl]pyridine (L) complexes containing inorganic salts with compositions, $[(L)Cu(H_2O)(C_2O_4)(H_2O)Cu(L)]C_2O_4$ (**1**), $[(L)Cu(H_2O)(C_3H_2O_4)(H_2O)Cu(L)]C_3H_2O_4$ (**2**), $[(L)Cu(H_2O)(C_4H_4O_4)(H_2O)Cu(L)]C_4H_4O_4$ (**3**), $[(L)Cu(H_2O)(C_8H_4O_4)(H_2O)Cu(L)]C_8H_4O_4$ (**4**), $[(L)Cu(H_2O)(ImH)(H_2O)Cu(L)](ImH)_3$ (**5**), $[(L)Cu(H_2O)(2\text{-}MeImH)(H_2O)Cu(L)](2\text{-}MeImH)_3$ (**6**), $[(L)Cu(H_2O)(2\text{-}EthImH)(H_2O)Cu(L)](2\text{-}EthImH)_3$ (**7**), $[(L)Cu(H_2O)(BenzImH)(H_2O)Cu(L)](BenzImH)_3$ (**8**) and $[(L)Cu(H_2O)(2\text{-}MeBenzImH)(H_2O)Cu(L)](2\text{-}MeBenzImH)_3$ (**9**) (Where C_2H_4 = Sodium Oxalate, $C_3H_2O_4$ = Sodium Malonate, $C_4H_4O_4$ = Sodium Succinate, $C_8H_4O_4$ = Sodium Terephthalate, ImH = Imidazole, 2-MeImH = 2-Methylimidazole, 2-EthImH = 2-Ethylimidazole, BenzImH = Benzimidazole and 2-MeBenzImH = 2-Methylbenzimidazole) have been synthesized and characterized for their spectroscopic and redox properties. In addition, SOD mimetic activities of these complexes have also been investigated.

Experimental

Synthesis of complex $[(L)Cu(H_2O)(C_2O_4)(H_2O)Cu(L)]C_2O_4$ 1

To a stirred solution (20 mL) of ligand (0.274 g, 1 mmol) was added $CuCl_2.2H_2O$ (0.170 g, 1 mmol) in methanol (10 mL) while stirring. To this reaction mixture, sodium oxalate (0.134 g, 1 mmol) in methanol (10 mL) was added drop-wise and refluxed for 1 hrs. After 1 hrs refluxing, the resulting reaction mixture was cooled at room temperature and filtered. The filtrate was allowed to evaporate slowly in the air. After 2-3 days microcrystalline powder was separated, this was collected upon filtration and stored in a calcium chloride desiccator. Yield: ~ 76 %. Anal. Calc. for $C_{38}H_{32}Cu_2N_8O_{10}$ (887.81 g mol^{-1}): C, 51.41; H, 3.63; N, 12.62 %. Found: C, 51.40; H, 3.60; N, 12.61 %. FTIR bands (KBr, cm^{-1}): 1613 ν(C=O), 1578 ν(C=N). ESI-Mass (m/z): 887.54.

Similarly, all other complexes were synthesized the synthetic route of all complexes is given below.

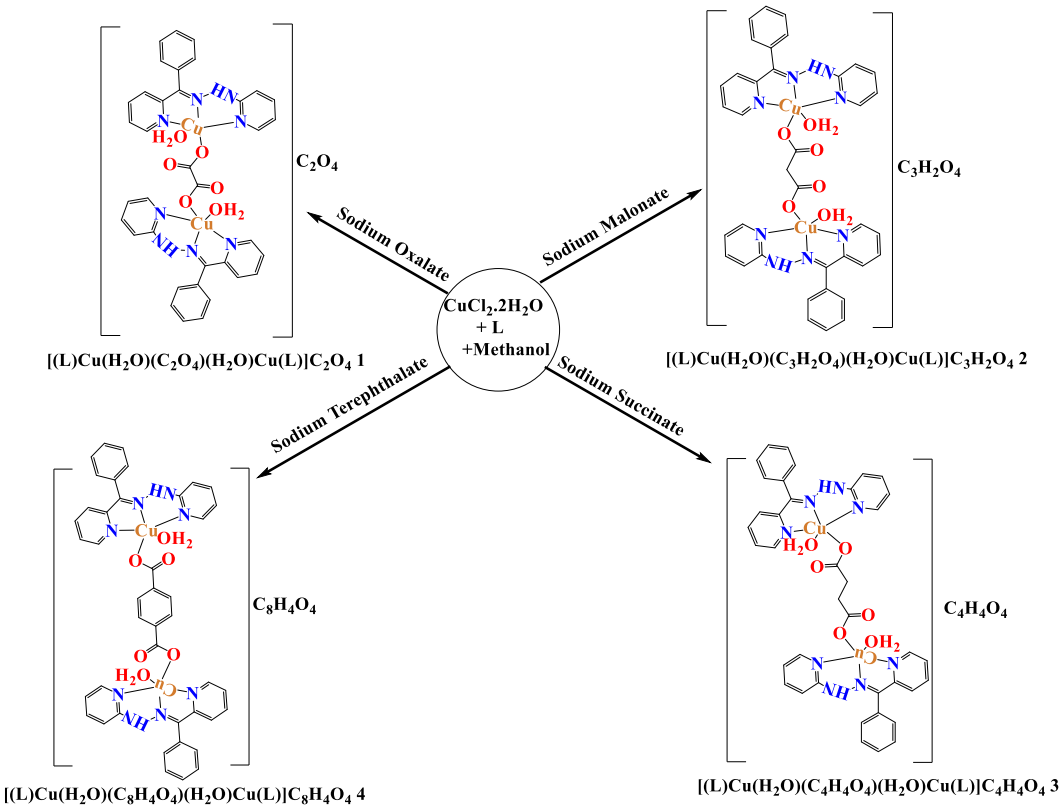

Scheme 1 Synthetic route of complexes **1-4**.

The structural formula of these complexes (**1-9**) is based on elemental analysis, spectroscopic FTIR, UV-Vis and epr data. The NMR spectra of the ligand are discussed in detail in this chapter part (A) section. However, crystals for X-ray analysis of complexes (**1-9**) could not be isolated even by recrystallization efforts. These complexes are air-stable. The solubility of all the nine synthesized complexes in DMF and DMSO is very high while partially soluble in $CHCl_3$ and CH_2Cl_2 and insoluble in water.

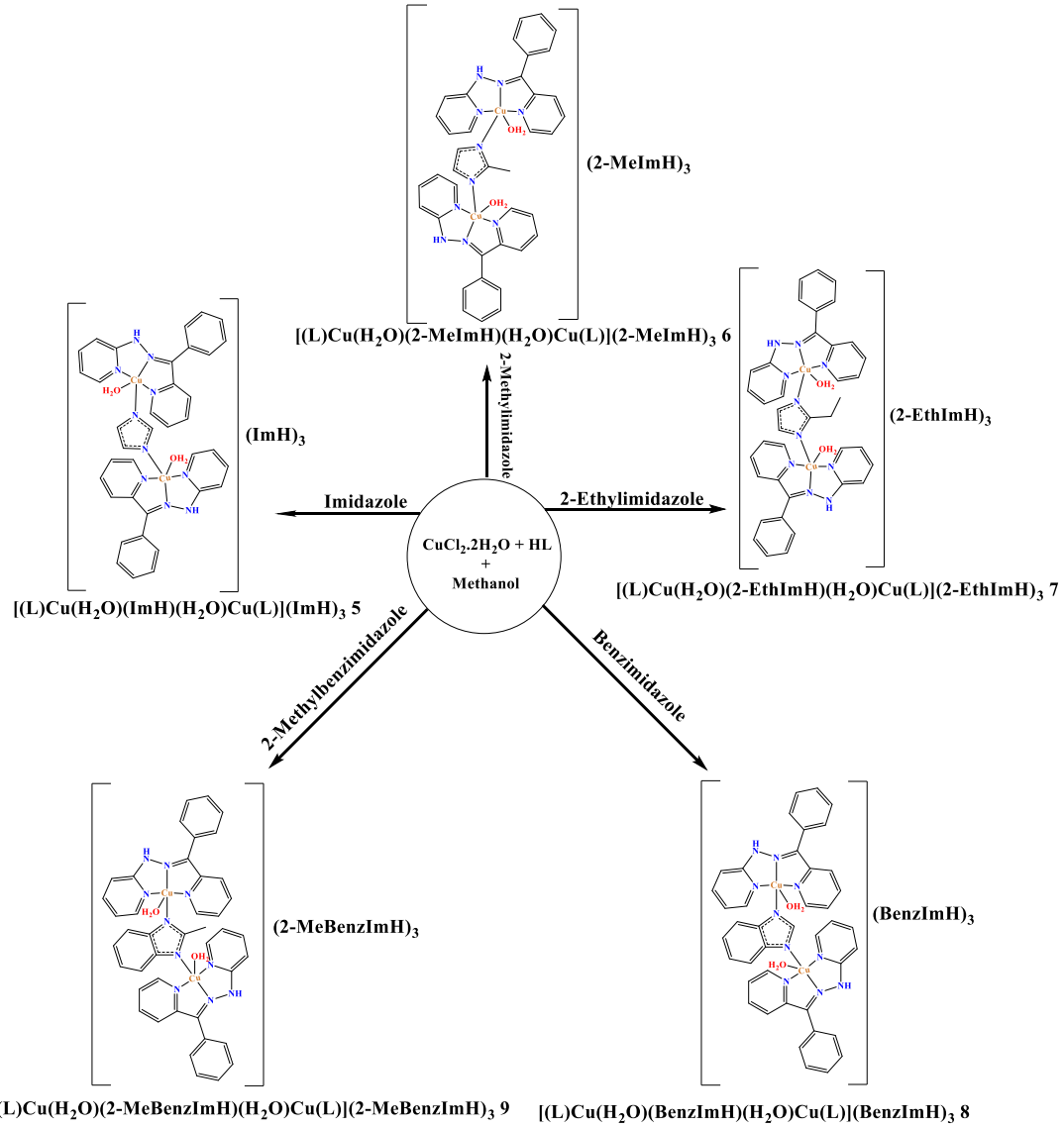

Scheme 2 Synthetic route of complexes **5-9**.

FTIR spectroscopy

An FTIR spectral study of all nine copper(II) was performed to get a basic idea about the coordination sites of the ligand and the compared with that of metal complexes and the peaks which have been changed due to complexation with metal ion is interpreted.

Some important bands of FTIR spectra of complexes **1-9**.

Compounds	ν(NH)	ν(OH)	ν(>C=O)	ν(>C=N)	ν(N-N)	ν(Cu-O)	ν(Cu-N)
HL	3084			1592	988		
1		3289	1613	1578	1068	472	419
2		3233	1625	1533	1089	542	479
3		3107	1603	1580	1026	542	479
4		3061	1612	1545	1108	435	419
5		3424		1564	1003	466	419

6		3442		1564	1004	467	419
7		3425		1564	1002	464	419
8		3408		1563	1001	418	411
9		3421		1563	1002	418	411

Electronic spectra

The electronic absorption spectral data λ_{max} (nm) of **1-9** in DMSO (1.0×10^{-3}M).

Compound	$\pi - \pi^*$	$d_{xz}, d_{yz} \rightarrow d_{x^2-y^2}$	$d_{xy} \rightarrow d_{x^2-y^2}$
1	379	486	701
2	377	486	701
3	325	485	704
4	378	486	702
5	325	490	ill-defined
6	325	491	ill-defined
7	324	491	ill-defined
8	325	491	ill-defined
9	322	491	725

Epr Studies

Epr spectral parameters of copper(II) complexes **1-9**.

Epr parameters	1	2	3	4	5	6	7	8	9
Polycrystalline state(298 K)									
$g_{\parallel}$	2.248	2.171	2.097	2.177	2.158	2.150	2.166	2.154	2.170
$g_{\perp}$	2.079	2.045	2.045	2.073	2.046	2.045	2.045	2.047	2.047
G	3.203	3.950	2.239	2.471	3.680	3.459	3.833	3.512	3.751
D(cm^{-1})	0.027	0.018	0.018	0.032	0.016	0.015	0.018	0.017	0.018
DMSO(77 K)									
$g_{\parallel}$	2.233	2.179	2.199	2.222	2.181	2.189	2.179	2.178	2.172
$g_{\perp}$	2.066	2.051	2.057	2.066	2.066	2.050	2.055	2.065	2.072
$A_{\parallel}$	155	167	175	160	160	163	165	172	169

Electrochemical studies

Summary of electrochemical in (V) data **1-9**.

Compound	E_{pc1}	E_{pc2}	E_{pa1}	E_{pa2}	DE_{pc1}	DE_{pc2}	ΔD_{pc}	$E_{1/2}{}^{1}$	$E_{1/2}{}^{2}$	$\Delta E_{1/2}$	K_{con}
1	-1.174		-0.475		-0.846			-0.824			
2	-1.067		-0.470		-0.801			-0.768			
3	-0.923		-0.299		-0.779			-0.611			
4	-0.315	-1.041	+0.240	-0.281	+0.324	-0.113	0.437	-0.034	-0.661	0.661	3.948×10^{10}
5	-0.635		-0.031		-0.655			-0.333			
6	-1.030		-0.411		-0.523	-0.774	0.251	-0.720			
7	-0.982		-0.502		-0.528	-0.758	0.230	-0.742			
8	-0.608	-1.025	-0.038	-0.491	-0.534	-0.79	0.256	-0.323	-0.758	0.435	2.248×10^{7}
9	-0.651	-0.993	-0.038	-0.534	-0.576	-0.790	0.214	-0.344	-0.763	0.419	1.205×10^{7}

Computational study of complexes

Quantum chemical analyses for complexes **1-9** were carried out to deduce quantitative relationships of the theoretical descriptors with the superoxide antioxidant relationship activity by using density functional theory calculations at B3LYP/LANL2DZ level.

Antioxidant superoxide dismutase (SOD) activity

The antioxidant SOD activity IC_{50} and kinetic catalytic constant for complexes **1-9**.

Compound	IC_{50} (μmol)	SOD activity (μmol^{-1})	k_{M_cCF} $(molL)^{-1}s^{-1}$ x 10^4	References
$[Cu_1L^1Im]$	2.5	-	-	111
$[CuZnL^1Im]$	30	-	-	111
$[Na_2Cu_4Na_2(TACNTA)_4.(H_2O)_6].(H_2O)_{26}$	1.08 M	-	-	112
$[Cu_2(\mu SCN)_2L^2{}_2]$	24	41.66	13.86	40
$[Cu(L^2)(HL^2)][Cu(L)(HL^2)]ClO_4.H_2O$	55	18.8	6.05	77
$[Cu(L^2)(NO_3)(\mu$-2-aminopyrazine$)Cu(L^2)(NO_3)].2H_2O$	15	66.67	22.17	77
Vc	852	1.17	0.39	113
1	25	40	13.30	This work
2	40	25	8.32	This work
3	30	33.33	11.08	This work
4	50	20	6.65	This work
5	24	41.67	13.86	This work
6	40	25	8.32	This work
7	38	26.31	8.75	This work
8	42	23.80	7.92	This work
9	25	40	13.30	This work

Conclusions

In this chapter we have synthesised nine binuclear complexes by using NNN (L = 2-[(E)-phenyl(pyridine-2-yl-hydrazono)methyl]pyridine) containing inorganic salts with compositions, $[(L)Cu(H_2O)(C_2O_4)(H_2O)Cu(L)]C_2O_4$ (**1**), $[(L)Cu(H_2O)(C_3H_2O_4)(H_2O)Cu(L)]C_3H_2O_4$ (**2**), $[(L)Cu(H_2O)(C_4H_4O_4)(H_2O)Cu(L)]C_4H_4O_4$ (**3**), $[(L)Cu(H_2O)(C_8H_4O_4)(H_2O)Cu(L)]C_8H_4O_4$ (**4**), $[(L)Cu(H_2O)(ImH)(H_2O)Cu(L)](ImH)_3$ (**5**), $[(L)Cu(H_2O)(2\text{-}MeImH)(H_2O)Cu(L)](2\text{-}MeImH)_3$ (**6**), $[(L)Cu(H_2O)(2\text{-}EthImH)(H_2O)Cu(L)](2\text{-}EthImH)_3$ (**7**), $[(L)Cu(H_2O)(BenzImH)(H_2O)Cu(L)](BenzImH)_3$ (**8**) and $[(L)Cu(H_2O)(2\text{-}MeBenzImH)(H_2O)Cu(L)](2\text{-}MeBenzImH)_3$ (**9**). These complexes have been characterized by various physicochemical techniques. The Geometry optimized structures of complexes **1-9** were carried out using density functional theory calculations at B3LYP/LANL2DZ level. In these binuclear complexes, each copper(II) centre has distorted square pyramidal and distorted trigonal pyramid geometry. These complexes also show good antioxidant activity.

Chapter: 4

Copper(II) hydrazone complexes with different nuclearties and geometries: Synthesis, structure, spectral properties, electrochemical behaviour, density functional study and *in vitro* catalytic activity

Quantum chemical parameters derived from Density functional theory (DFT) calculations were employed as a physiochemical description of the complexes. DFT has vast applications in the development of the quantitative structure-activity relationship (QSAR) for the explanation of enzymatic and superoxide dismutase activity study. The theoretical parameters utilized are composed of energies of highest occupied molecular orbital (HOMO), energies of lowest unoccupied molecular orbitals (LUMO) energy gap (ΔE), ionization potential (I), electron affinity (EA), electronegativity (χ), chemical potential (μ), global hardness (η), softness (S), electrophilicity index (ω), electron-donating capacity (ω-) and electro accepting capacity (ω+). All these electronic parameters are analyzed and discussed. To the best of our knowledge with [HL= (Z)-N´-{(2-hydroxynapthalen-1-yl}methylene)acetohydrazide] copper(II) complexes have not been reported systematically until present work. Therefore, to explore the behaviour of copper(II) complexes with naphthyl hydrazone ligand with or without co-ligands we have focused the synthetic approach which persuade binary, mixed ligands and binuclear complexes. This chapter describes syntheses and structural characterization of nine copper(II) complexes with different nuclearties and geometries using tridentate hydrazone [HL= (Z)-N´-{(2-hydroxynapthalen-1-yl}methylene)acetohydrazide] *viz.*, $[Cu(HL)(OH_2]ClO_4$ **1,** $[Cu(HL)(OH_2)]ClO_4$ **2,** $[Cu(HL)(OH_2)]NO_3$ **3,** [Cu(HL)(Cl)] **4,** $[Cu(HL)(DMPHEN)]ClO_4$ **5,** [Cu(HL)(BZI)].CH_3OH **6,** $[(HL)Cu(\mu\text{-}ClO_4)Cu(L)(2H_2O)]$ **7,** $[(HL)Cu(\mu\text{-}SO_4)Cu(HL)(2H_2O)]$ **8** and $[(HL)Cu(\mu\text{-}bpm)Cu(HL)](ClO_4)_2.3H_2O$ **9 (**where DMPHEN = 2, 9-dimethyl-1,10-phenanthroline, BZI = benzimidazole and bmp = 2,2-Bipyrimidine).

The molecular structures of the newly synthesized complexes were evaluated using the single-crystal X-ray diffraction technique. The crystal structures confirmed the composition and geometry as proposed by other physicochemical methods. These complexes were further analyzed by Hirshfeld surfaces and fingerprint plots to assess the intermolecular interactions in the crystalline structures of complexes. The observed interactions have been discussed in detail. All complexes were further characterized by microanalysis, ultraviolet-visible (Uv-vis),

infrared (IR) and electron paramagnetic resonance (epr) spectroscopy. The complexes were also studied using electrochemical (cyclic and differential pulse voltammetry) techniques. The DFT calculations were also performed to support the experimental findings. Bioactivity (catalytic) measurements have also been done and findings discussed.

Synthesis of Ligand (HL)

Schiff base ligand HL = N'-((2-hydroxynaphthalen-1-yl) methylene) acetohydrazide was synthesized by taking a solution of 2-hydroxy-1-napthaldehyde (1.50 g, 10.00 mmol) and acetyl hydrazide (0.65 g, 10.00 mmol) in ethanol (50 mL) with few drops of glacial acetic acid as a catalyst was refluxed for 1 hrs. The Schiff base was isolated from the resulting yellow solution. The obtained solid product from the solution was washed with cold ethanol and kept in a $CaCl_2$ desiccator.

Yield: 83 %. Anal. Cal. for $C_{13}H_{12}N_2O_2$ (228.25 g mol^{-1}): Calc. C, 68.41; H, 5.30; N, 12.27 %; Found C, 68.42; H 5.32; N, 12.29 %. FTIR (KBr, cm^{-1}) 3441 ν(OH), 3185 ν(N-H), 1672 ν(C=O), 1643 ν(C=N). ^{1}H NMR (DMSO-d_6) δ: 12.6 (s, 1H, OH), 11.7 (s, 1H, NH), 9.1 (s, 1H, CH=N), 7.1-8.9 (d/t, 6H, napth-H), 2 (s, 3H, CH_3) ppm. ^{13}CNMR δ: 171.5 (C-OH), 165.7 (C=O), 145.1 (-CH=N-), 108.9-132.9 (m, 9C, naphtha-C), 21.8 (-OCH_3) ppm.

2.2.2 Synthesis of the complex $[Cu(HL)(OH_2]ClO_4$ 1 and $[Cu(HL)(OH_2]ClO_4$ 2

To a 20 mL methanolic solution of $Cu(ClO_4).6H_2O$ (0.370 g, 1.00 mmol) and the HL (0.228, 1.00 mmol) was added with two to three drops of triethylamine. The reaction mixture was stirred for 3 hrs and filtered. The filtrate was divided into two equal parts. One of the parts was left at room temperature for evaporation and the other was kept in a refrigerator (~10 °C). Blue coloured single crystals of **1** were obtained after one week from the filtrate which was left at room temperature, whereas dark blue single crystals of **2** were obtained after one month from the other part of the filtrate which was kept in the refrigerator. Crystals of both parts were collected upon filtration and dried in $CaCl_2$ desiccators.

Complex **1**, Yield; ~ 83 %. Anal. Calc. for $C_{13}H_{13}ClCuN_2O_7$ (408.24 g mol^{-1}): Elemental Analysis: C, 38.25; H, 3.21; N, 6.86 %; Found: C, 38.27; H, 3.19; N, 6.84 %. Conductance (Λ_m/s cm^2 mol^{-1}) in DMSO 120. FTIR bands (KBr, cm^{-1}): ν(C=O) 1617, ν(C=N) 1598.

Complex **2**, Yield; ~ 82 %. Anal. Calc. for $C_{13}H_{13}ClCuN_2O_7$ (408.25 g mol^{-1}): Elemental Analysis: C, 38.25; H, 3.24; N, 6.86 %; Found: C, 38.24; H, 3.20; N, 6.82 %. Conductance (Λ_m/s cm^2 mol^{-1}) in DMSO 130. FTIR bands (KBr, cm^{-1}): ν(C=O) 1618, ν(C=N) 1597.

Similarly, all other complexes were synthesized.

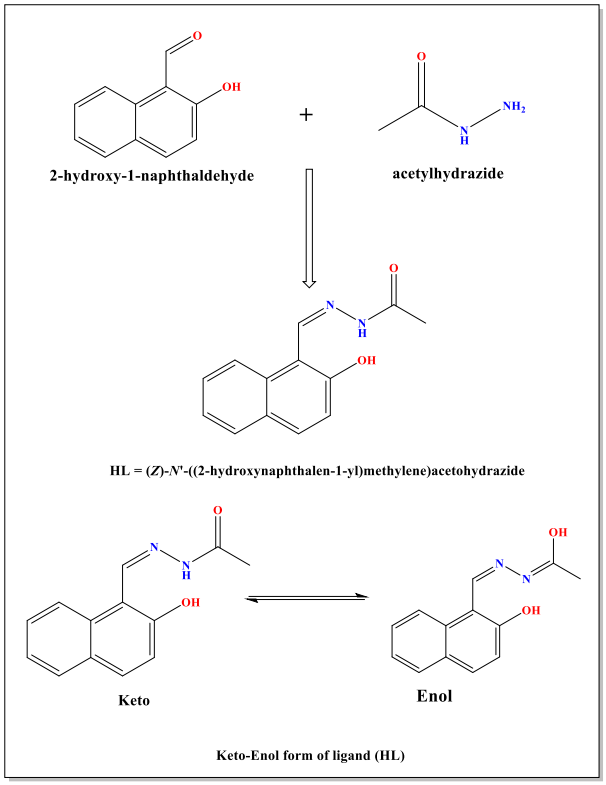

Scheme 1 Synthetic route of the ligand.

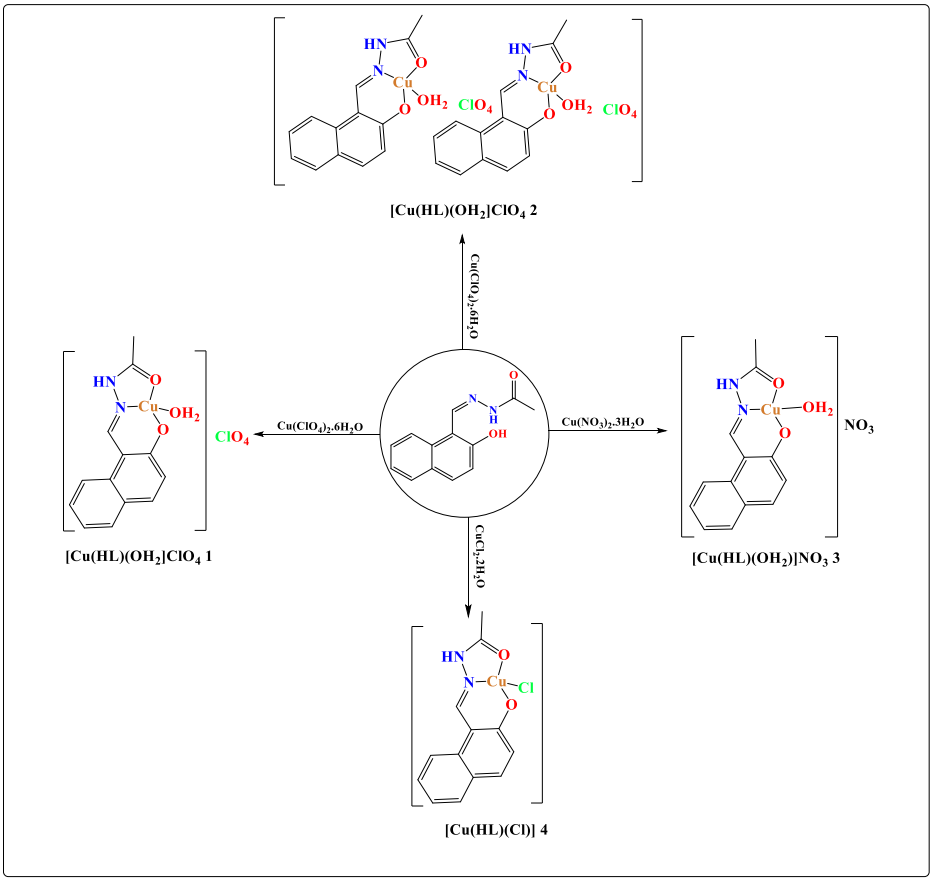

Scheme 2 Synthetic route of mononuclear complexes **1-4**.

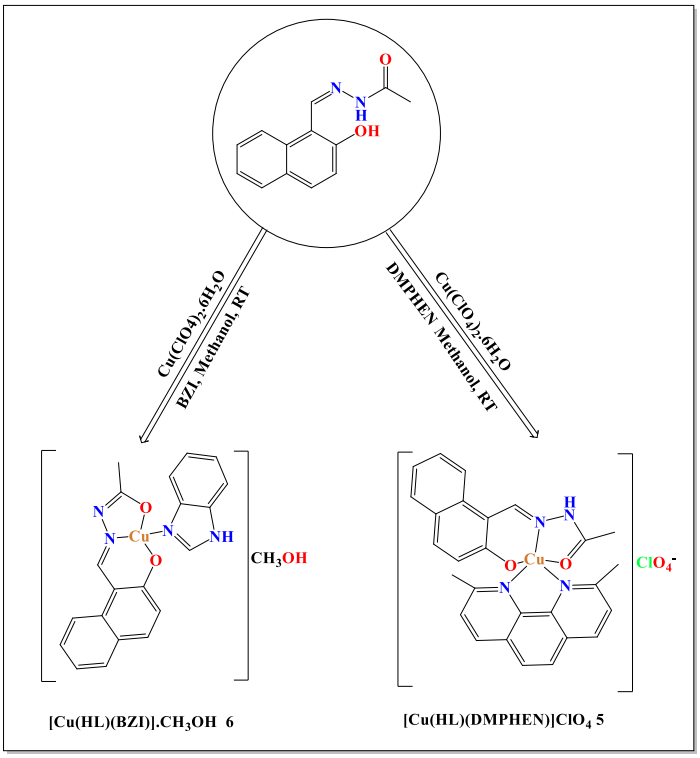

Scheme 3 Synthetic route of mixed ligand complexes **5** and **6**.

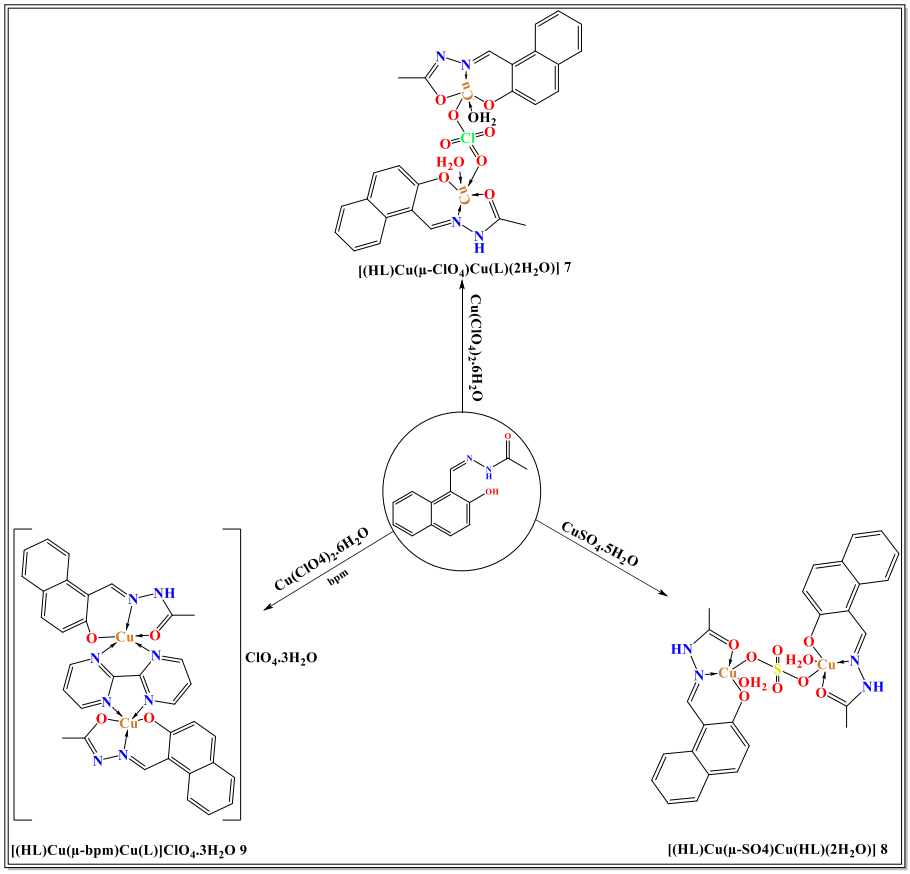

Scheme 4 Synthetic route of binuclear complexes **7-9**.

FTIR studies

Important frequencies of FTIR spectral data.

Compounds	ν(C=O)	ν(C=N)	ν(M-O)	ν(M-N)
HL	1672	1643	- - -	- - -
1	1617	1598	493	441
2	1618	1597	492	439
3	1618	1578	491	447
4	1592	1516	469	434
5	1616	1601	476	459
6	1622	1590	456	437
7	1617	1599	457	423
8	1618	1606	456	427
9	1631	1572	511	477

Crystal Structures

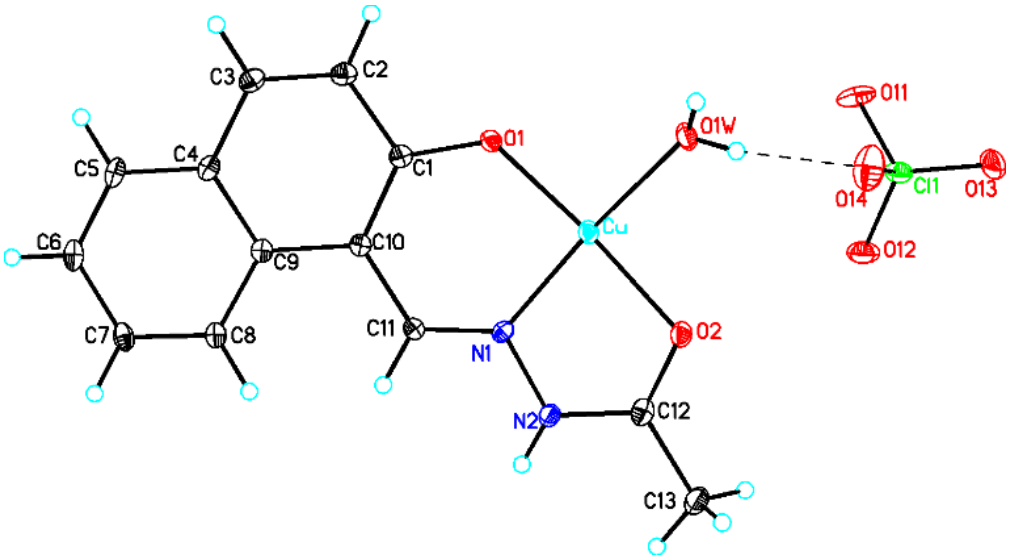

Fig. 13. ORTEP view of complex **1**.

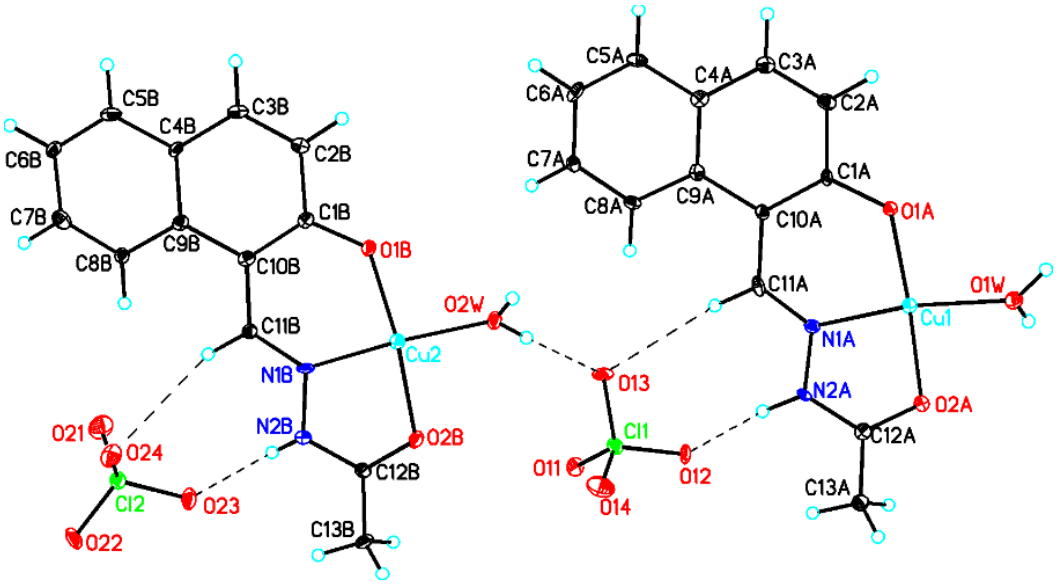

Fig. 14. ORTEP view of complex **2**(dimeric view).

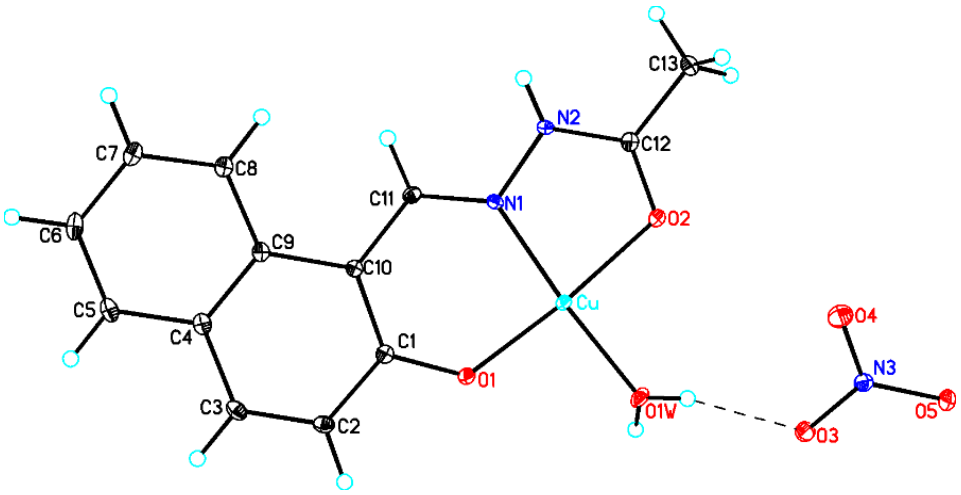

Fig. 15. ORTEP view of complex **3**.

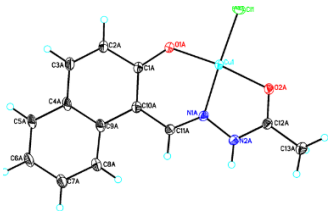	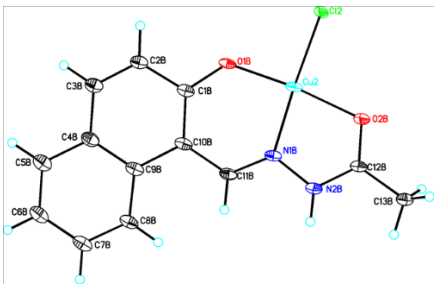
(a)	**(b)**

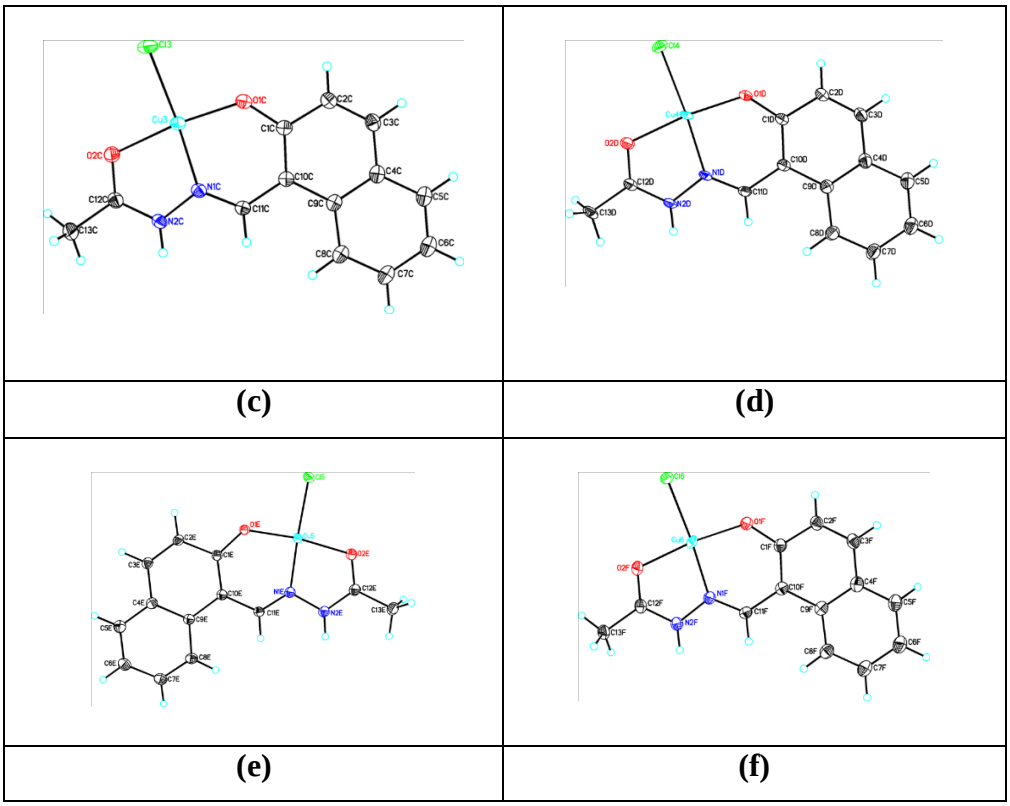

(c) **(d)**

(e) **(f)**

Fig. 16. ORTEP view of complex **4** six containing six units (hexameric view) ((**a**)-(**f**)).

Hirshfeld Surface Analysis (HSA)

HAS is performed for all complexes**.**

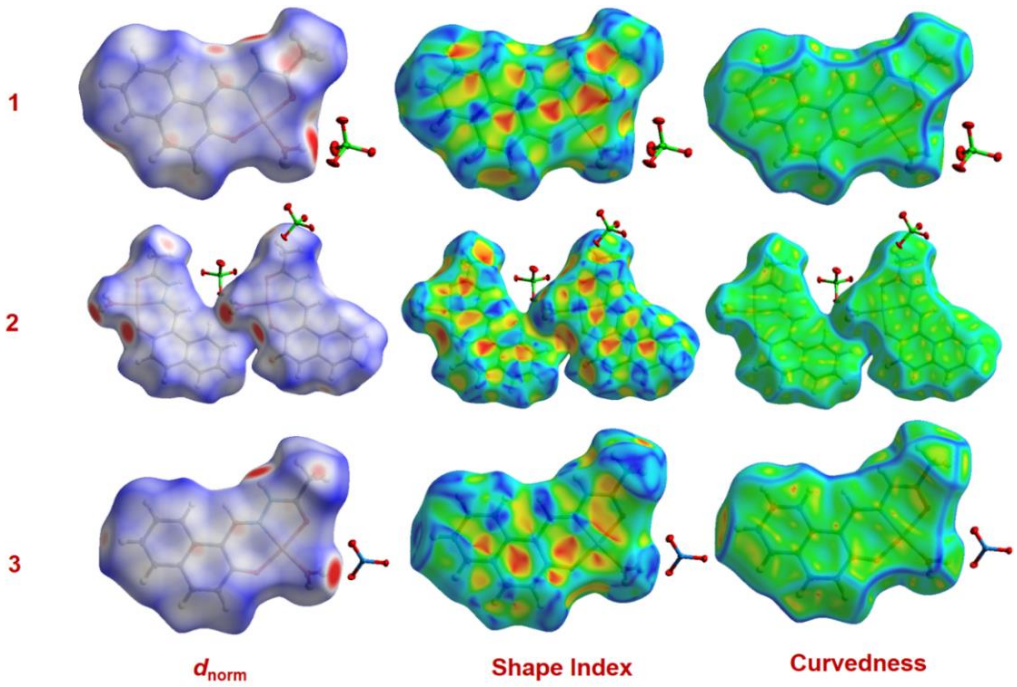

Hirshfeld surfaces mapped with d_{norm}, shape index and curvedness for **1-3**.

Electronic and Electrochemical studies of complexes

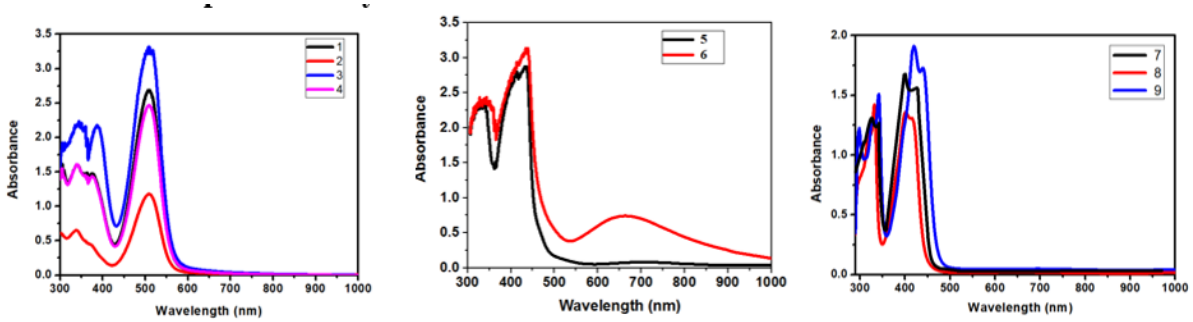

The electronic spectra of complexes have been measured in DMSO solution (3.0×10^{-4} M).

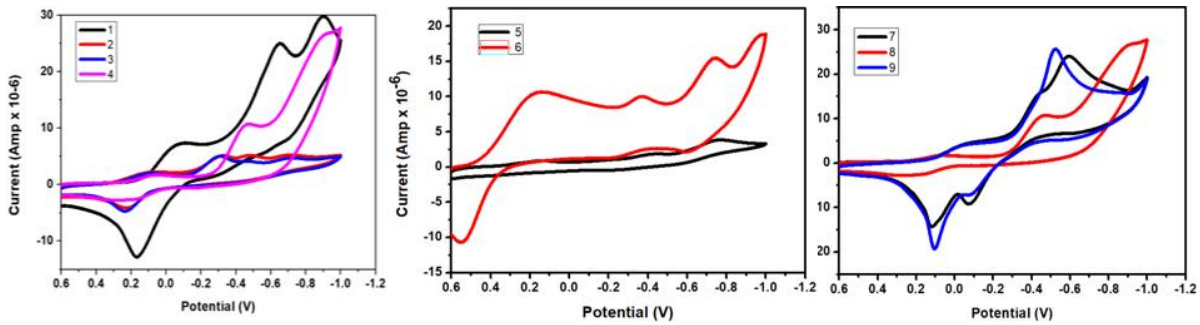

CV of complexes **1-9.**

Conclusions

In summary, we have synthesized and characterized nine copper(II) complexes with tridentate hydrazone (HL) ligand. Molecular structures of all complexes have been determined using single-crystal X-ray diffraction techniques. The Hirshfeld analysis and the fingerprint plots revealed how much the weak CH···π and π ···π non-covalent interactions lead both complexes to build supramolecular architectures. The paramagnetic behaviour of both complexes has been explored using magnetic and X-band epr spectral study. The electrochemical stability of the metal center was investigated using cyclic and differential pulse voltammetry. Time-Dependent Density functional theory (TD-DFT) calculations throw light on electronic transitions. Finally, SOD activity data of both complexes collected at pH 7.4 using the NBT assay method. Finally, SOD activity measurements manifest that these complexes are good models with outstanding catalytic activity towards the dismutation of $O_2^{\cdot-}$.

References

1 G.J. Brewer, J. Am. Coll. Nutr. 28 (2009) 238–242.
2 K.G. Daniel, P. Gupta, R.H. Harbach, W.C. Guida, Q.P. Dou, Biochem. Pharmacol. 67 (2004) 1139–1151.
3 S. Puig, D.J. Thiele, Curr. Opin. Chem. Biol. 6 (2002) 171–180.
4 I. Persson, P. Persson, M. Sandstrom, A.-S. Ullstrom, J. Chem. Soc. Dalton Trans. 7 (2002) 1256-1265.
5 M.A. Halcrow, Dalton Trans. (2003) 4375-4384.
6 S. Keinan, D. Avnir, Inorg. Chem. 40 (2001) 318-323.
7 D.G. Barceloux, D. Barceloux, Clin. Toxicol. 37 (1999) 217-230.
8 R.R. Conry, Encyclopaedia of Inorganic Chemistry, John Wiley and Sons, Ltd. (2006) 1-19.
9 G. Tamasi, L. Chiasserini, L. Savini, A. Sega, R. Cini, J. Inorg. Biochem. 99 (2005) 1347-1359.
10 S. Banarjee, A. Ray, S. Sen, S. Mitra, D.L. Hughes, R.J. Butcher, S.R. Batten, D.R. Turner, Inorg. Chim. Acta 361 (2008) 2962-2700.
11 S. Banerjee, S. Sen, S. Basak, S. Mitra, D. L. Hughes, C. Desplanches, Inorg. Chim. Acta 361 (2008) 2707-2714.
12 P.E. Aranha, M.P.D. Santos, S. Romera, E.R. Dockal, Polyhedron 26 (2007) 1373-1382.
13 P.V. Bernhardt, P. Chin, P.C. Sharpe, J.Y.C. Wang, D.R. Richardson, J. Biol. Inorg. Chem. 10 (2005) 761-777.
14 B. Bottari, R. Maccari, F. Monforte, R. Ottana, E. Rotondo, M.G. Vigorita, Bioorg. Med. Chem. Lett. 10 (2000) 657-660.
15 J. Easmon, G. Puerstinger, T. Roth, H.H. Fiebig, M. Jenny, W. Jaeger, G. Heinisch, J. Hofmann, Int. J. Cancer 94 (2001) 89-96.
16 D.S. Kalinowski, P.C. Sharpe, P.V. Bernhardt, D.R. Richardson, J. Med. Chem. 51 (2008) 331-344.